



Norwegian University
of Life Sciences

Master's Thesis 2021 60 ECTS

Faculty of Chemistry, Biotechnology and Food Science (KBM)

Effect of Microbial Metabolites on Mitochondrial Function in Colonocytes

Karen Sivertsen Utheim

MSc Chemistry and Biotechnology

Effect of Microbial Metabolites on Mitochondrial Function in Colonocytes

The Norwegian University of Life Sciences (NMBU),
Faculty of Chemistry, Biotechnology and Food Science

©Karen Sivertsen Utheim, 2021

Acknowledgements

The work presented in this thesis was performed at two laboratories. The RNA work was carried out at Faculty of Chemistry, Biotechnology and Food Science at Norwegian University of Life Sciences, under the supervision of Professor Knut Rudi. The cell work and respirometry was performed at Institute of Clinical Medicine at University of Oslo under the supervision of Professor Lars Eide.

First of all, I would like to express my gratitude to my main supervisor Knut Rudi and my co-supervisor Lars Eide. The opportunity to work at the intersection between your fields of research have been truly special. I am honored to have had the guidance of two dedicated scientists and appreciate the enthusiasm and encouragement you have shown throughout the entire process. It has left me with invaluable knowledge and experience.

I am also very grateful for the help I received from Ragnhild Skinnes, Ida Ormaasen and Morten Nilsen. With everything from instructions in the lab to answers to all my questions along the way, you have always shown great patience and positivity. Along with the rest of the staff and students at both labs, you have also provided a fun and inclusive environment that made me look forward to every day in the lab.

Last but not least, thanks to my family and friends for all the love and support you provide. In particular, I would like to thank the awesome people of “Rappkjefta Ryper”. I could not have wished for a better group of friends during these years. Even when careers and pandemic have brought us apart, you continue to brighten my day with your humor and compassion.

Ås, January 2021

Karen Sivertsen Utheim

Abstract

The colonocytes are the most abundant cell type in the colonic epithelium and function both as a barrier and a mediator between the human body and the components in the gut lumen, such as the microbiota and its metabolites. In particular, the gut microbiota produces the short chain fatty acids (SCFA): acetate, propionate and butyrate, with butyrate being the colonocytes preferred energy source. Branched chain fatty acids (BCFA) are major constituents of vernix caseosa and human milk, and are therefore consumed by the fetus and the infant. The aim of this study was to investigate the effects these two groups of fatty acids have on colonocytes.

Caco-2 cells were used as a colonocyte model and the cells were treated with either 4 mM SCFA or 40 μ M BCFA. RNA-sequencing was used to identify genes and pathways influenced by the fatty acids. Butyrate showed most effect on the gene expression, and the associated pathways were related to regulation of the cell cycle. Propionate was the second most influential treatment on the gene expression and shared some of the effects observed with butyrate. The mitochondrial activity of the cells was assessed by measuring gene expression and respiration. Both SCFA and BCFA had impact on mitochondrial activity, but the effects differed between the groups. The results from butyrate-treated cells indicated a shift from glycolysis to β -oxidation, while 15-methylhexadecanoic acid seemed to increase the cells respiratory capacity. The concentration of BCFA was measured in the fecal samples from 176 infants at 12 months of age in the PreventADALL cohort. The most abundant fatty acid measured was 12-methyltetradecanoic acid, and 14-methylhexadecanoic acid was the least abundant.

In conclusion, the results of this study suggest that butyrate is the fatty acid that have most impact on the cells but also that propionate may play an important role in the infant gut, particularly when butyrate concentrations are low. The observed effects of the BCFAs also demonstrate that these fatty acids should be considered when deciphering the infant development. However, the study was limited to investigating fatty acids individually and at a single concentration. Further work is therefore needed to elucidate the biologic function of the fatty acids in the infant gut.

Sammendrag

Kolonocyttene er den mest utbredte celletypen i epitelet i tykktarmen og fungerer både som en barriere og et bindeledd mellom kroppen og innholdet i tarmen, som mikrobiotaen og metabolittene den produserer. Mikrobiotaen produserer spesielt de kortkjedede fettsyrene eddiksyre, propionsyre og smørsyre, hvorav smørsyre er den foretrukne energikilden til kolonocyttene. Forgrenede fettsyrer utgjør en stor andel av vernix caseosa og morsmelk, og konsumeres derfor av både foster og spedbarn. Formålet med denne studien var å undersøke effekten kortkjedede og forgrenede fettsyrer har på kolonocyttene.

Caco-2-celler ble brukt som en modell for kolonocytter og ble behandlet med 4 mM SCFA eller 40 μ M BCFA. RNA-sekvensering ble brukt til å identifisere gener og reaksjonsveier som påvirkes av fettsyrene. Smørsyre førte til mest effekt på genuttrykket, og reaksjonsveiene som ble identifisert var involvert i reguleringen av cellesyklus. Propionsyre var den behandlingen med nest mest påvirkningskraft, og den hadde noen av de samme effektene som ble observert med smørsyre. Den mitokondrielle aktiviteten i cellene ble vurdert ved å måle genuttrykk og respirasjon. Både kortkjedede og forgrenede fettsyrer påvirket den mitokondrielle aktiviteten, men med ulikt utfall. Cellene som ble behandlet med smørsyre ga resultater som indikerte en overgang fra glykolyse til β -oksidasjon, mens 15-metylheksadekansyre viste tegn til å øke cellenes respirasjons-kapasitet. Konsentrasjonen av forgrenede fettsyrer ble malt i avføringsprøver fra 176 spedbarn på 12 måneder i PreventADALL-kohorten. Fettsyren med høyest median-konsentrasjon var 12-metyltetradekansyre, og 14-metylheksadekansyre hadde lavest median-konsentrasjon.

Oppsummert, viser resultatene fra denne studien at smørsyre er den fettsyren som har størst påvirkning på cellene, men at propionsyre også kan spille en viktig rolle i tarmen hos spedbarn, spesielt når konsentrasjonen av smørsyre er lav. Effektene av de forgrenede fettsyrene understreker også at disse bør inkluderes i utredningen av spedbarns utvikling. Begrensninger ved studien var at fettsyrene kun ble undersøkt enkeltvis og bare ved en konsentrasjon. Videre arbeid er derfor nødvendig for å beskrive funksjonen disse fettsyrene har i tarmen hos spedbarn.

Abbreviations

12-MTD	12-methyltetradecanoic acid
13-MTD	13-methyltetradecanoic acid
14-MHD	14-methylhexadecanoic acid
15-MHD	15-methylhexadecanoic acid
ATP	Adenosine triphosphate
AMPK	AMP-activated protein kinase
BCFA	Branched chain fatty acid
BER	Base excision repair
CPM	Counts per Million
DE	Differentially expressed
DMEM	Dulbecco's modified Eagle's essential medium
DMSO	Dimethyl sulfoxide
DNA	Deoxyribonucleic acid
ETC	Electron transport chain
ETF:QO	Electron transferring flavoprotein-ubiquinone oxidoreductase
FBS	Fetal bovine serum
FCCP	Carbonyl cyanide-p-trifluoromethoxyphenylhydrazone
GC	Gas chromatograph
GI	Gastrointestinal
GOI	Gene of interest
GPCR	G-protein-coupled receptor
HDAC	Histone deacetylase
IEC	Intestinal epithelial cell
mRNA	Messenger ribonucleic acid
PCR	Polymerase chain reaction
qPCR	Quantitative polymerase chain reaction
RNA	Ribonucleic acid
ROS	Reactive oxygen species
RPKM	Reads Per Kilobase of transcript per Million
rRNA	Ribosomal ribonucleic acid
SCFA	Short chain fatty acid
TCA	Tricarboxylic acid
TPM	Transcripts per Million

Innholdsfortegnelse

1	Introduction	1
1.1	<i>Gut epithelial cells</i>	2
1.2	<i>Short chain fatty acids</i>	2
1.3	<i>Branched chain fatty acids</i>	4
1.4	<i>Mitochondrial metabolism</i>	5
1.5	<i>Methods involved to assess cell responses</i>	7
1.5.1	Colonocyte Model	7
1.5.2	Gene expression	8
1.5.3	Respirometry	10
1.6	<i>Aim of thesis</i>	13
2	Materials and methods	14
2.1	<i>Cell culture</i>	15
2.1.1	Maintenance of cell culture	15
2.1.2	Detachment of cells from plate surface	15
2.1.3	Estimation of cell number	15
2.2	<i>Cell characterization</i>	15
2.3	<i>Fatty acid-treatment</i>	16
2.4	<i>Cell respiration</i>	16
2.5	<i>Gene expression</i>	17
2.5.1	RNA extraction	17
2.5.2	DNase treatment	17
2.5.3	RNA quantification and qualification	17
2.5.4	cDNA synthesis	18
2.5.5	qPCR	18
2.6	<i>RNA-sequencing</i>	19
2.6.1	Library preparation	19
2.6.2	Library normalization and validation	20
2.7	<i>In vivo concentrations of branched chain fatty acids</i>	20
2.8	<i>Data analysis</i>	21
2.8.1	Relative quantification of qPCR gene expression	21
2.8.2	Gene expression using RNA-sequencing	21
2.8.3	Pathway analysis	23
2.8.4	Statistical analysis	23
3	Results	25
3.1	<i>Establishment of in vitro system</i>	25
3.2	<i>Gene expression using RNA-seq</i>	26
	Differentially expressed transcript variants	27
	Pathways associated with the differentially expressed genes	28
3.3	<i>Gene expression by qPCR</i>	30
3.4	<i>Respiration</i>	33
3.5	<i>Verification of BCFA concentrations</i>	35
4	Discussion	36
4.1	<i>Differentially expressed genes and associated pathways with fatty acid treatments</i>	36
4.1.1	Effect on gene expression by butyrate and propionate	36

4.1.2	Impact on the cell cycle regulation by butyrate-treatment.....	36
4.1.3	Activation of cellular responses to stress.....	37
4.2	<i>The influence on mitochondrial activity by fatty acids</i>	38
4.2.1	A shift in respiration with butyrate-treatment.....	38
4.2.2	The effect on respiration by propionate-treatment.....	39
4.2.3	Indications of increased mitochondrial activity by BCFA-treatment.....	40
4.3	<i>The use of Caco-2 cells as a colonocyte model</i>	40
4.3.1	Respirometry measurements at different cell densities.....	40
4.3.2	Cell model limitations.....	41
4.4	<i>Methodological considerations of gene expression quantification</i>	42
4.4.1	RNA-seq as a high-throughput method for gene expression screening.....	42
4.4.2	qPCR relative quantification by endogenous control.....	44
4.5	<i>Physiologic relevance of fatty acid concentrations used in treatment of Caco-2 cells</i>	45
4.5.1	SCFA treatment concentrations.....	45
4.5.2	In vivo BCFA concentrations in the infant gut.....	46
5	Value of results and future work	47
6	References	48
	Appendix A: RNA qualification	58
	Appendix B: Primer Efficiencies	59
	Appendix C: Correlations between controls in RNA-seq	60
	Appendix D: Differentially expressed transcripts/genes	61
	Appendix E: Top pathways with propionate-treatment	66
	Appendix F: In vivo fatty acid concentrations	67

1 Introduction

It has become increasingly apparent that the human body is not a desolate island but a densely populated metropolis of microorganisms, collectively called the microbiota. The gastrointestinal (GI) tract consist of a surface of 250-400 m² of the human body that constantly interact with organisms and components from the environment (Thursby & Juge, 2017). In particular, the colon provides an environment that is well suited for microorganisms because of the availability of nutrients, long transit time and close to neutral pH (Flint et al., 2012b). This part of the GI tract harbors inhabitants from all of the three taxonomic domains; Bacteria, Archaea and Eucarya.

The microbiota has been co-evolving with their hosts over millions of years, leading to the complex symbiosis experienced today. This relationship proves to be of significant importance to the host health. The commensal bacteria provide functions such as protecting against pathogens, providing energy for host cells and shaping the human immune system (Kamada et al., 2013; Milani et al., 2017). The colonization of the infant gut is a process of ecological succession and the composition of microorganisms changes drastically during the first years of life (Lozupone et al., 2012). The process is influenced by factors such as mode of delivery, feeding and administration of pharmaceuticals such as antibiotics (Milani et al., 2017). An adult-like microbiota starts to develop as the infant is introduced to solid foods and stabilizes around the age of 2,5 to 3 years. The process is characterized by a shift from facultative to obligate anaerobes, as the anaerobic environment typical for the healthy adult gut is established (Albenberg et al., 2014; Friedman et al., 2018).

The exact composition of bacterial species in the adult gut varies between healthy individuals (Lozupone et al., 2012). However, the functional diversity in the gut is smaller between individuals than the phylogenetic diversity (Abubucker et al., 2012). Turnbaugh et al. (2009) suggest that there is a collection of shared microbial genes that provide functions that are important for the host. This means that even though different bacterial species make up the microbiota in different individuals, similar bacterial proteins and metabolites are present (Thursby & Juge, 2017).

By turning of available substrates into metabolites, the microbiota has a substantial effect on the host. The nutrients that reach the colon are in particular complex carbohydrates such as

dietary fibers and resistant starch that the human enzymes are unable to process (Ferreyra et al., 2014). This also includes human milk oligosaccharides (HMOs) in infants fed with breastmilk, that are important nutrition for the microbiota as they are not digested or absorbed by the infant (Milani et al., 2017). Together with some remaining simple carbohydrates and mucin produced by the secretory epithelial cells in the gut, these serve as sustenance for the gut microbiota (Chassard & Lacroix, 2013). Collectively, the microbiota yields a diverse arsenal of enzymes to tackle these substrates and produce fatty acids, amino acids and vitamins that are absorbed and metabolized by the human cells (Flint et al., 2012a; Hill, 1997).

1.1 Gut epithelial cells

The intestinal epithelial cells (IEC) function as a barrier between the ecosystem in the lumen and the rest of the human body. Neighboring cells are connected to each other by junctions, creating a continuous layer (Peterson & Artis, 2014). The IEC secrete mucin and antimicrobial peptides, but also absorb substances from the lumen (Correa-Oliveira et al., 2016). The cells are involved in the tolerance and immune reactions towards the bacteria in the lumen through production of cytokines (Peterson & Artis, 2014).

Multipotent stem cells reside in the crypts of the colon and differentiate into absorptive colonocytes, or secretory cells such as enteroendocrine cells, goblet cells, and tuft cells (Noah et al., 2011). Colonocytes are the most abundant of the colonic epithelial cells and as they mature, they migrate up the crypt-lumen axis. The differentiation process is accompanied by a metabolic shift from glycolysis to β -oxidation (Duszka et al., 2017; Lefebvre et al., 1999). This leads to higher oxygen consumption and is therefore important for maintaining the anaerobic conditions in the lumen (Litvak et al., 2017). The mature colonocytes perform a range of important functions, such as electrolyte exchange, detoxification and synthesis of mucin, lipids and structural proteins (Ahmad et al., 2000).

1.2 Short chain fatty acids

Of the microbial metabolites in the gut, the SCFAs are of particular interest. Obligate anaerobic bacteria in the gut specialize in metabolizing complex carbohydrates into short chain fatty acids (SCFA) (Litvak et al., 2018). A broad diversity of bacteria, dominated by

SCFA producers, is associated with a balanced and homeostatic microbiota (Byndloss et al., 2017). The SCFA butyrate is the colonocytes preferred source of energy (Roediger, 1980). SCFAs are characterized by having less than six carbons and the most abundant SCFAs produced by bacteria in the colon, are acetic acid, propionic acid and butyric acid (Rios-Covian et al., 2016). The measured proportions between acetate, propionate and butyrate vary, but have a mean molar ratio of 60:20:20 in adults (Hamer et al., 2008). The infant gut is predominated by acetate and propionate, butyrate being almost absent at the beginning of life, but SCFA proportions and total amount vary with breast-feeding status (Bridgman et al., 2017). The relative proportions of the different SCFAs change a lot during the first year and the butyrate concentration increases with age (Norin et al., 2004).

While most of the butyrate is used by the colonocytes upon absorption, acetate and propionate reach the circulation and are transported to other parts of the body (Macfarlane & Macfarlane, 2007). Acetate is utilized by the brain, heart and peripheral tissues, and interact with the body's handling of fat and lipids by increasing satiety and browning of white adipose tissue (Lavelle & Sokol, 2020). Propionate is metabolized by the liver and can be processed to obtain glucose through gluconeogenesis (Bergman, 1990).

The presence of SCFA protects against pathogenic microorganisms by lowering the pH and increasing production of antimicrobial peptides (Correa-Oliveira et al., 2016). In addition to this, butyrate stimulates mucin production and lowers the bacterial adhesion in the gut (Jung et al., 2015). The activation of AMP-activated protein kinase (AMPK) and stabilization of the hypoxia-inducible factor (HIF) by butyrate leads to reassembly of tight junctions and enhanced tissue barrier (Kelly et al., 2015; Peng et al., 2009). Absence of butyrate can induce apoptosis in the colonocytes and leads to deterioration of the mucosa (Orchel et al., 2005). SCFA is associated with positive effects on the immune responses such as protection from colitis and colitis-induced cancer (Lavelle & Sokol, 2020).

The mechanisms through which the SCFA influence the host cells are by activation of G-protein-coupled receptors (GPCRs) and inhibition of histone deacetylases (HDACs) (den Besten et al., 2015; Miao et al., 2016). The GPCRs activated by SCFA are important in regulation of immunity and may be central in development of tolerance by inducing regulatory T-cell (T_{reg}) production (Smith et al., 2013; Sun et al., 2017). When HDACs are inhibited, the histones that participate in the packing of DNA into chromatin remain

acetylated (Miao et al., 2016; van der Knaap & Verrijzer, 2016). The acetylation neutralizes the positive charge of histone tails, weakening the bond to the negatively charged DNA (Li & Reinberg, 2011). A looser packing of the chromatin leaves the DNA more available for transcription. This mechanism influence the expression of a number of genes and has antiproliferative effect on cancer cells (Davie, 2003).

1.3 Branched chain fatty acids

Branched chain fatty acids (BCFA) are fatty acids that are reported at low levels in internal tissues of humans, but are suspected to be of nutritional importance in infants due to its rich presence in vernix caseosa and human milk (Ran-Ressler et al., 2013). These fatty acids carry one or more methyl branches, usually near the end of the carbon chain (Ran-Ressler et al., 2013). If the methyl group is situated on the penultimate carbon, the fatty acid is called iso-BCFA. Similarly, a methyl group on the antepenultimate carbon creates an anteiso-BCFA.

BCFA are significant components of membranes in bacteria, and similar to unsaturated fatty acids, they are used to control membrane fluidity (Kaneda, 1991; Siliakus et al., 2017). However, because they are saturated, they do not react with oxygen (Dingess et al., 2017). BCFA are produced from the branched chain amino acids valine, leucine and isoleucine which are essential amino acids that the human body is unable to produce. Bacteria produce both the relevant amino acids and branched fatty acids. Kaneda (1991) lists species from 56 genera where BCFA constitutes more than 20 % of the total cellular fatty acids. The percentage is particularly high in *Bacilli* and *Lactobacilli* species, as well as some *Bifidobacteria* strains which all can inhabit the gut (Ran-Ressler et al., 2014).

The vernix caseosa that surrounds normal term infants at birth has an abundance of BCFA (Ran-Ressler et al., 2013). The vernix is suspended in the amniotic fluid and is swallowed by the fetus nearing term birth. There is a difference in the estimated amount of BCFA swallowed by the fetus and the measured amount of BCFA in meconium, which indicates that the BCFA is absorbed and metabolized by the fetal gut. Increased risk for necrotizing enterocolitis (NEC) in premature infants is assumed to be related to lack of BCFA due to less vernix ingestion (Ran-Ressler et al., 2011). Most non-vegan adults consume food containing BCFA such as dairy and meat products, as well as some fermented foods (Ran-Ressler et al., 2014). The seven major BCFA in food are *iso-14:0*, *iso-15:0*, *anteiso-15:0*, *iso-16:0*, *iso-17:0*,

anteiso-17:0, *iso*-18:0 (Hauff & Vetter, 2010). Dingess et al. (2017) report that half of the BCFA in dairy products from cow is *anteiso*-15:0 and *anteiso*-17:0. BCFA is also present in human milk, but the contribution to this by endogenous production versus supply from the diet or the microbiota have not been elucidated (Dingess et al., 2017). Research on groups of mothers that consume little BCFA containing food suggest that the fatty acids in the breast milk may, at least to some degree, come from the maternal microbiota (Dingess et al., 2017).

Despite its low concentrations in adult tissue, the presence of BCFA in the body have been associated with effects on human health and metabolism, such as having anti-inflammatory effects (Yan et al., 2017). A link has also been suggested between obesity and lower BCFA concentrations in serum and adipose tissue, and BCFA is suggested to have positive influence on insulin sensitivity (Taormina et al., 2020). Little is known about mechanisms behind the observed effects of BCFA on the human health.

1.4 Mitochondrial metabolism

The human body obtains energy from proteins, lipids and carbohydrates (Da Poian et al., 2010). The most important energy carrier in the body is adenosine triphosphate (ATP), where energy is stored in the bonds between phosphate groups (Dunn & Grider, 2020). The majority of ATP is produced in the mitochondria, by the process of oxidative phosphorylation.

Different reactions deliver reducing power to the electron transport chain (ETC) in the form of the molecules NADH and FADH₂. If the terminal electron acceptor oxygen is unavailable, some ATP can be produced through fermentation, but the full potential of the nutrient will not be realized, as the end product is lactate instead of the completely oxidized CO₂ (Mathews et al., 2013).

Glucose is broken down to pyruvate by the process of glycolysis in the cytosol, and some ATP and NADH are generated. In the mitochondrial matrix, the pyruvate molecule is decarboxylated by pyruvate dehydrogenase (PDH) into Acetyl-CoA that enter the tricarboxylic acid (TCA) cycle. This process reduces nicotinamide adenine dinucleotide (NAD⁺) and flavin adenine dinucleotide (FAD) to respectively NADH and FADH₂, producing some ATP and releasing CO₂ (Mathews et al., 2013). Fatty acids are transported across both the mitochondrial membranes and broken down, two carbons at the time, in the β -oxidation process (Ma et al., 2018). Each round of oxidation produces FADH₂, NADH and

Acetyl-CoA. Nutrient availability influence the metabolic state of the cell through transcription factors and remodeling of chromatin structure which regulate the expression of metabolic enzymes (van der Knaap & Verrijzer, 2016).

The reducing equivalents produced in the TCA cycle and β -oxidation contribute to ATP production by the ETC as illustrated by figure 1.1. NADH is re-oxidized to NAD^+ by NADH dehydrogenase (complex I) and FADH_2 is re-oxidized by succinate dehydrogenase (complex II) or electron transferring flavoprotein-ubiquinone oxidoreductase (ETF:QO) (Nicholls & Ferguson, 2002). Electrons from these oxidations are transferred to ubiquinone (Q) and protons are pumped into the intermembrane space, creating a proton gradient across the inner membrane of the mitochondrion. Electrons are transferred to the final electron acceptor oxygen by cytochrome c oxidase (complex IV), reducing O_2 to H_2O . The ATP-synthase (complex V) transports protons back into the matrix, using the proton gradient as the driving force to produce ATP (Acín-Pérez et al., 2008). The consumption of oxygen is therefore tightly linked to the production of ATP.

Complex I and ubiquinone-cytochrome c reductase (complex III) in the ETC produce reactive oxygen species (ROS) that can damage the deoxyribonucleic acid (DNA) (Turrens, 1997). The mitochondrial DNA encode several components of ETC, and the metabolic activity is affected if ROS damage is not efficiently repaired. The main repair mechanisms for DNA damage in the mitochondria is base excision repair (BER), initiated by glycosylases such as 8-oxoguanine glycosylase (OGG1) that detect one of the most common DNA damages (Van Houten et al., 2018). BER genes are up-regulated in response to increased oxidative damage to the DNA (Rusyn et al., 2004).

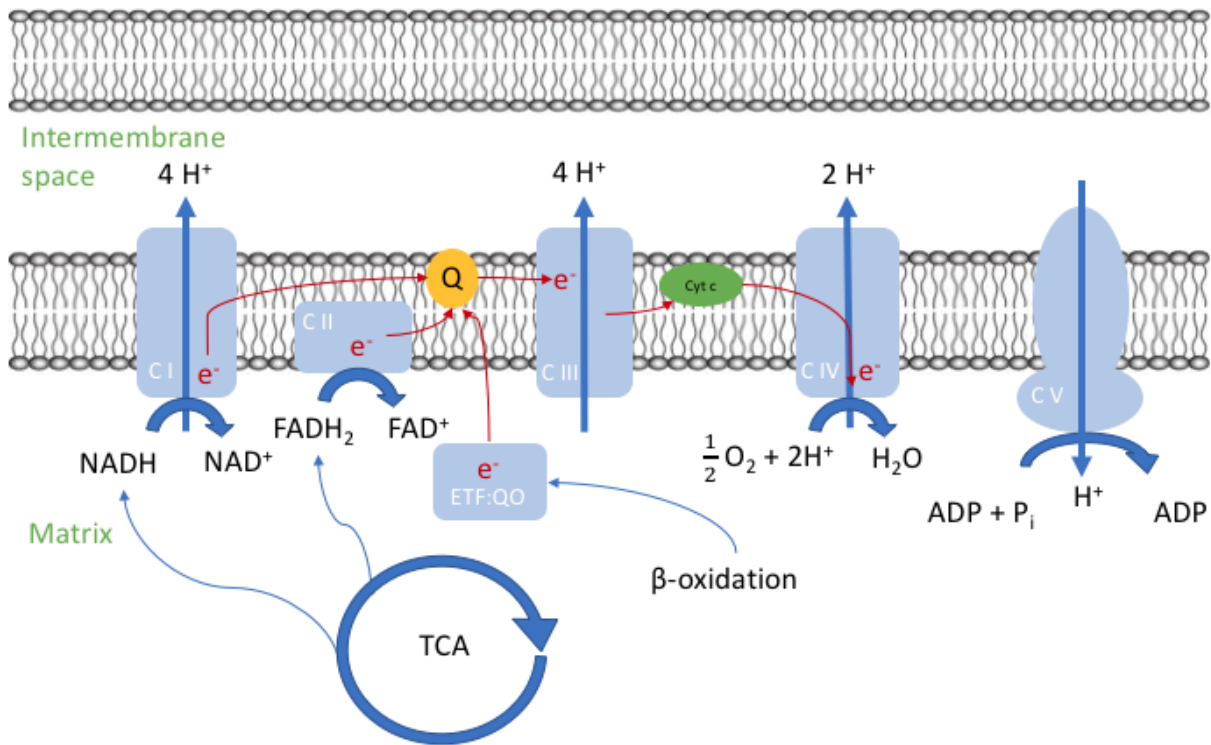


Figure 1.1 The electron transport chain and ATP synthase (complex V) situated in the inner mitochondrial membrane, and how it is supplied by reduced electron carriers by the TCA cycle and β -oxidation. Figure made by inspiration from Mathews et al. (2013) and Scialo et al. (2017).

1.5 Methods involved to assess cell responses

Cells have a complex system for adapting to changes in their environment. Proteins are the main performers of cellular functions and the amount of different proteins are for the most part regulated by how many mRNAs are transcribed from the genome. The use of cell models provides a simplified system for studying effects of different treatments. Gene expression measurements give an overview of the processes in the cell and can say something about which pathways are involved in the adaptation to a treatment. To elucidate how the sum of pathways manifests in cellular activities, techniques focused at the functions performed by the cells are better suited. Respirometry is a method used to estimate the cells mitochondrial activity.

1.5.1 Colonocyte Model

Caco-2 is a colorectal cancer cell line that grow in a monolayer and can differentiate according to cell density (Pignata et al., 1994). Levy et al. (1995) have described three states of differentiation in vitro for the Caco-2 cells; At subconfluence, the cells are homogeneously

undifferentiated. Up to 20 days of postconfluence, the cells are heterogeneously differentiated with varying morphology of the cells and development of a brush border. At 30 days postconfluence, the cells reach a state of homogenous polarization and differentiation. The differentiation leads to columnar absorptive cells (Zweibaum, 1991). The Caco-2 cells have a closest resemblance to colonocytes immediately after confluence and the resemblance to the small-intestinal enterocyte increase after this point (Engle et al., 1998).

1.5.2 Gene expression

Measurements of the gene expression of a cell sample is done by quantifying the amount of RNA transcribed from different genes. This requires the RNA to be isolated from the cells and turned into complementary DNA (cDNA). By designing primers targeting specific genes, gene expression of known GOIs can be measured using qPCR. RNA-seq is a method that enables assessment of the complete transcriptome of the sample.

RNA extraction

The nucleic acids can be extracted from cell samples by wide range of different methods, depending on the start material and the downstream applications (Ali et al., 2017). Some of the issues the extraction process needs to handle is to get sufficient amount of nucleic acids, and to avoid contaminations of other cellular components or reagents that may interfere with downstream applications. The sample also has to be free of nucleases as these degrade the nucleic acids. The ribonucleic acid (RNA) is particularly unstable, partly due to the abundance of RNases present in the environment (Tan & Yiap, 2009).

To access the nucleic acids, the cell membranes needs to be destroyed. This is done by chemical, enzymatical or mechanical disruption (Burden, 2012). A method to separate the desired nucleic acid from the other cellular components, is by solid phase extraction where the nucleic acids bind to the solid phase such as columns with silica membrane, or magnetic beads under the right conditions. Numerous kits for nucleic acid extraction are available. They are specifically developed for a certain cell type and the nucleic acid of interest.

Gene expression analysis using quantitative PCR (qPCR)

The polymerase chain reaction (PCR) makes it possible to amplify a specific DNA fragment from a sample of DNA (Garibyan & Avashia, 2013). This is done by repeated cycles of

denaturation, annealing and elongation that leads to exponential increase of the target sequence. The end-point amount of PCR product is however not a reliable estimate of the input amount of the fragment. This is because the rate of amplification will decrease when the reaction runs out of one of the reaction components, and the amount of amplicons in an experiment will usually reach a plateau of about the same level (Kubista et al., 2006). By using fluorophores that bind non-specifically to dsDNA, the amount of DNA can be measured in real-time during the process. This method is called quantitative PCR (qPCR). When the number of dsDNA strands in the solution increase, the dye will bind to them and emit a fluorescent signal that increase proportionally with the dsDNA molecules. The amount of the targeted DNA originally in the sample can be estimated by evaluating the number of cycles needed to reach a certain threshold level of fluorescent signal (Kubista et al., 2006). A higher amount of template at the starting point will require fewer cycles to reach the threshold. By transforming isolated RNA to cDNA, this technology can be used to measure the expression level of genes in a sample.

Gene expression can be quantified by qPCR in an absolute or relative manner. Absolute quantification is dependent on having a dilution series of a sample with a known number of transcripts of the gene of interest (GOI) (Boulter et al., 2016). Relative quantification can be done by comparing the gene expression of a GOI to that of a reference gene in the same sample (Arya et al., 2005). This is usually a housekeeping gene that shows constant expression under different conditions. The gene of the glycolytic enzyme glyceraldehyde-3-phosphate dehydrogenase (GAPDH) is one of the genes that have commonly been used. A gene is valid as reference in an experiment if amplification efficiencies and abundance of GOI are approximately the same as reference, and the reference is equally expressed between different treatments (Boulter et al., 2016).

RNA-sequencing

While PCR-based methods provide a cost- and labor effective way to measure gene expression of a limited number of GOIs, the sequencing technology has opened a new world of possibilities when it comes to examining cellular processes. RNA-sequencing enables studies of the whole transcriptome, and the discovery of any gene showing differential expression between samples. The resulting information can also be used in a pathway analysis to reveal relevant processes. The development from sanger sequencing to next

generation sequencing has also made this a less time-consuming and more affordable alternative.

There are multiple species of RNA in human cells, but for gene expression studies, mainly the messenger RNA (mRNA) is of interest. mRNA make up less than 5% of the total RNA, while ribosomal RNA (rRNA) make up more than 80% (Westermann et al., 2012). If the library is prepared from the total collection of RNA, most of the reads will map to a few rRNA genes, resulting in a low coverage for the remaining, less abundant genes, such as the protein coding ones (Sims et al., 2014). To obtain a higher sensitivity for mRNA, the samples can be processed by either polyA⁺ selection or rRNA depletion in the library preparation (Zhao et al., 2018). The polyA⁺ selection method targets the polyadenylated tail of eukaryotic mRNA to isolate these from total RNA, also excluding non-polyA⁺ RNAs that have important functions (Zhao et al., 2014). This method lead to poor results on degraded RNA, as it only captures the part of the RNA with the polyA⁺ tail (Zhao et al., 2014). The rRNA depletion method uses hybridization capture to remove the rRNA molecules. This strategy results in libraries including more of the transcriptomic diversity, but has lower coverage of the exons as more reads map to intronic or intergenic regions (Zhao et al., 2018).

RNA is processed into a cDNA library, which is sequenced by Illumina or a similar high-throughput system. Sequencing produces reads from random positions on the RNA. Gene expression is measured by mapping the reads to a reference genome and counting the number of reads mapped to each gene (Finotello & Di Camillo, 2015), or more accurately each transcript variant, as eukaryotic cells rely on alternative splicing of genes to produce RNA (Black, 2003).

1.5.3 Respirometry

Oxygen is crucial as the terminal electron acceptor in oxidative phosphorylation and measuring the consumption of oxygen can give insight into the metabolic function of the cells. An oxygraph can be used to measure O₂ concentration in a sample of cells. The oxygraph-2K consist of two sample chambers, each equipped with a stirrer and a Clark electrode. The electrode consists of a platinum cathode covered by an oxygen-permeable membrane and a reference Ag/AgCl anode. The amperometric sensor measures the change in current between the cathode and the anode, when voltage is applied. The current is linearly

proportional to the number of O₂ molecules reduced at the cathode (Mendelson, 2012). The computer software reports the measured O₂-concentration as well as the change in concentration per time unit (O₂ flux).

Use of inhibitors and substrates to profile respiration capacity

Different inhibitors and substrates of the ETC complexes can be added to a cell sample while measuring the oxygen consumption rate to gain insight into the mitochondrial function of the sample (Brand & Nicholls, 2011). Figure 1.2 shows how bioenergetic profiling can be performed.

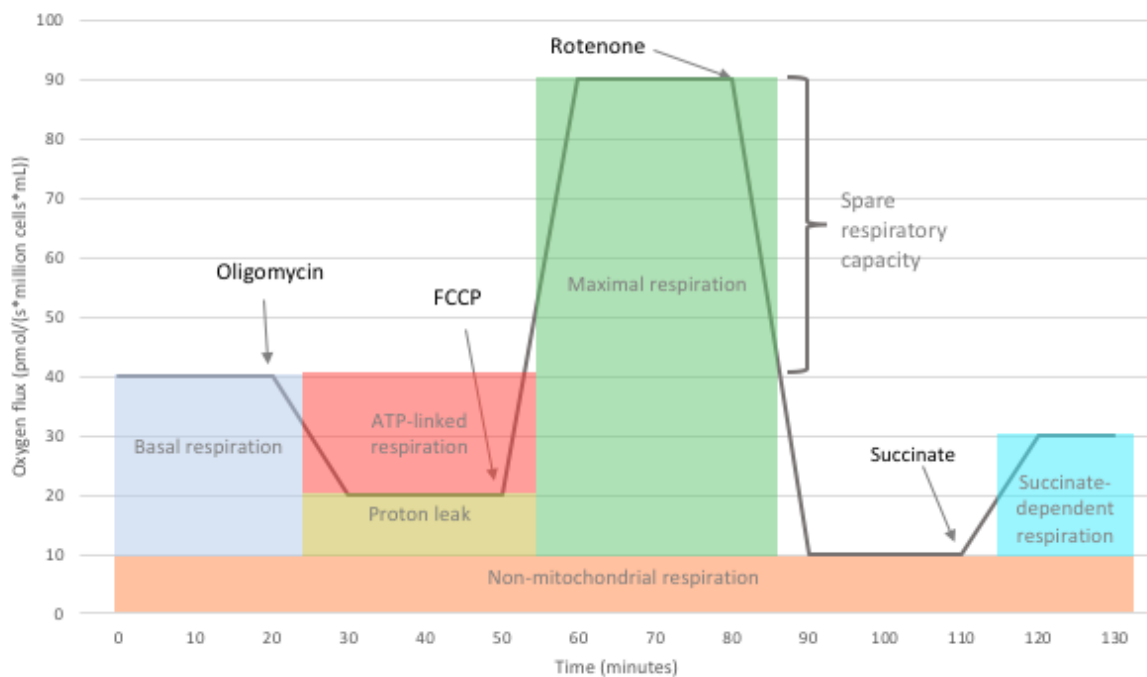


Figure 1.2 Bioenergetic profiling using respirometry. The addition of different inhibitors or substrates to a cell dispersion while measuring the concentration of oxygen leads to a change in the rate of oxygen consumption by the cells. This is used as a measure for the levels of basal, maximal, ATP-linked and succinate-dependent respiration. Figure adapted from Hill et al. (2012)

The basal respiration is the cells consumption of oxygen in an uninfluenced state. To reveal how much of the basal respiration that is used to generate ATP, oligomycin is added. Oligomycin is an antibiotic that binds to and inhibits ATP synthase, preventing protons from reentering the matrix of the mitochondria (Lee & O'Brien, 2010). In this state, the presence of ADP no longer stimulates an increase in respiration (Djafarzadeh & Jakob, 2017). In the

intact mitochondrion, the activity of the I to IV complexes is dependent on the activity of the last complex, the ATP synthase. If the protons are not pumped back into the matrix, the concentration will eventually be too high to energetically favor transporting protons into the intermembrane space, and the electron transport stops (Mathews et al., 2013). The remaining mitochondrial oxygen consumption is related to heat production due to proton leak (Gnaiger, 2019).

Carbonyl cyanide-4-trifluoromethoxyphenylhydrazone (FCCP) is a protonophore that increase the proton permeability of the inner membrane of the mitochondrion (Djafarzadeh & Jakob, 2017). It is added by titration to uncouple the respiration from the production of ATP. The protons are no longer required to go through complex V to reenter matrix, which means that the cells will continue to pump out protons and consume oxygen. Addition of FCCP therefore reveals the maximum respirational capacity of the cells.

Rotenone is a naturally occurring pesticide produced by several plant species (Betarbet & Greenamyre, 2008). It blocks the transfer of electrons between complex I and ubiquinone. This inhibits the activity of the ETC and reveals how much of the cells oxygen consumption that is not caused by the mitochondrial respiration, but by non-mitochondrial enzymes (Jang et al., 2016).

Succinate is a substrate for the enzyme succinate dehydrogenase which is both a part of the TCA cycle and the ETC, where it is a component of complex II (Bezawork-Geleta et al., 2017; Tretter et al., 2016). Succinate cannot be transported across the cell membrane (Ehinger et al., 2016), but a membrane-permeable form of succinate can be used in respirometry of intact cells. Complex II contain a flavoprotein subunit and similarly to ETF:QO deliver electrons to coenzyme Q. Measuring the respiration through complex II therefore also gives an estimate of the capacity for β -oxidation.

The ATP-linked respiration is represented by the difference between the non-phosphorylating respiration and the basal respiration. This is an estimate of how much of the respiration is dedicated to production of ATP which the cell may use for energy consuming activities. The spare respiratory capacity says something about the cells potential to increase the respiration if needed and is represented by the difference between the basal respiration and the maximal respiration (Jang et al., 2016).

1.6 Aim of thesis

Microbiota is known to have important impact on the host and much of the effects have been attributed to the metabolites produced by bacteria. Colonocytes are the hosts closest connection to the microbiota and they absorb SCFA and BCFA from the lumen. Colonocytes use the SCFA butyrate as the primary energy source, but there is a lack of knowledge regarding how the colonocytes respond to SCFA and BCFA.

Therefore, the main aim of this thesis was to measure the effect of physiologic concentrations of these fatty acids on a colonocyte model. To achieve this, the following sub-goals were included:

- Establish a colonocyte model.
- Investigate the effects of SCFA and BCFA on mitochondrial function in colonocytes.
- Identify cellular pathways influenced by the fatty acids.
- Determine concentrations of BCFA in the feces of 12-month-old infants from the PreventADALL (Prevent Atopic Diseases and Allergy) cohort.

2 Materials and methods

Work flow

The main part of this thesis consisted of an *in vitro* study of the effect of fatty acids on a gut epithelium cell model. The cells were treated with three SCFA and four BCFA at concentrations simulating the physiologic conditions in the gut lumen. The physiologic relevance of the concentrations of BCFA used to treat the cells were verified by measuring the concentrations in fecal samples from infants in the PreventADALL cohort. Figure 2.1 provides an overview of the performed experiments.

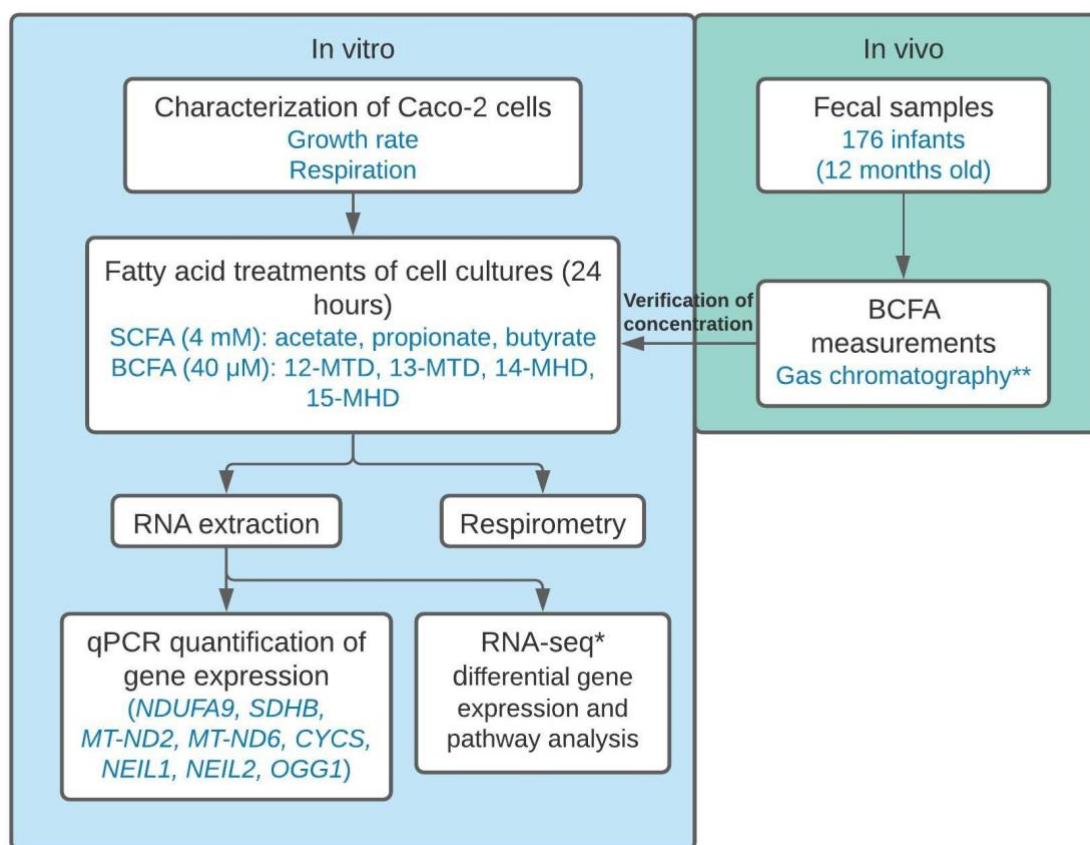


Figure 2.1 An overview of the experimental procedures involved in the thesis. Caco-2 cells were used to assess the effects of SCFA and BCFA on gene expression and the cellular respiration. The treatment concentrations for BCFA were verified by measuring the *in vivo* concentrations in fecal samples from the PreventADALL cohort.

* The sequencing was performed by Norwegian Sequencing Centre (Oslo).

** The GC was performed by Vitas (Oslo).

2.1 Cell culture

2.1.1 Maintenance of cell culture

The medium used were Dulbecco's modified Eagle's essential medium (DMEM) (Sigma-Aldrich, Norway) containing 25 mM (4500g/ml) glucose, added 10 % fetal bovine serum (FBS) and 1 % penicillin/streptomycin. The cultures were maintained in an incubator at 37 °C and 5 % CO₂. The medium was changed three times a week and the cultures were passaged at sub-confluence, two times a week.

2.1.2 Detachment of cells from plate surface

Each time the cultures were split or harvested, the cells were released by addition of trypsin. The medium was removed carefully, and the cells were rinsed with the same amount of PBS before trypsin was added. For handling T25, T75 or T175 cultures, 0,5, 1 and 3 ml of trypsin were used respectively. The cells were incubated at 37 °C with trypsin for 5 min and then collected in DMEM.

For harvesting cells from plates, 1 ml of trypsin was used. The cells were incubated with trypsin for 5 minutes and collected in DMEM. For further DNA and RNA analysis, the cell suspension was transferred to Eppendorf tubes, centrifuged and depleted of medium. The cell pellets were stored at -80 °C.

2.1.3 Estimation of cell number

To measure the number of cells in the cell dispersion, Countess Automated Cell Counter (Invitrogen, USA) was used. 20 µl of trypan blue was mixed with 20 µl of cell dispersion and 14 µl of the mixture was added to each chamber of a cell counting slide. A mean of the cell count readings of the two chambers was calculated and used as an estimate for the cell number.

2.2 Cell characterization

The Caco-2 cells were grown until 70 % confluence. Plates were prepared with DMEM and 3,0*10⁵ cells were added to each plate. The cultures were incubated at 37 °C and cells from two plates were harvested every 24 hours, for a total of 6 days. The cells were counted and analyzed by respirometry.

2.3 Fatty acid-treatment

Caco-2 cells were treated with either acetate, propionate, butyrate, 12-methyltetradecanoic acid (12-MTD) (*anteiso*-15:0), 13-methyltetradecanoic acid (13-MTD) (*iso*-15:0), 14-methylhexadecanoic acid (14-MHD) (*anteiso*-17:0) or 15-methylhexadecanoic acid (15-MHD) (*iso*-17:0) for 24 hours. Approximately $6,0 \cdot 10^5$ cells were added to each plate and grown in DMEM for four days before analysis and harvesting. The third day, the medium was removed and fresh medium containing fatty acids was added. The cells were treated for 24 hours before harvest and analysis.

The three types of SCFA were each dissolved in dH₂O to 10mg/ml and sterile filtered through a 0,2 µm filter. The fatty acid solution was added to DMEM to a concentration of 4 mM. 25 mg of BCFA were dissolved in 1 ml of DMSO and added to DMEM to a concentration of 40 µM. The medium was then sterile filtered, using a 0,2 µm filter.

2.4 Cell respiration

The respiration of suspended cell cultures was measured using a high-resolution Oxygraph-2K (Oroboros Instruments, Austria). The chambers held a temperature of 37 °C with stirring of 750 rpm. The data from the Oxygraph-2K was sampled every 2 seconds and recorded with the Datlab 7 software (Oroboros Instruments, Austria). Before each experiment was started the system was calibrated at air saturation by stirring media in the presence of air in the chambers until a stable signal was reached.

Cell samples suspended in medium, were initially left in the chambers to stabilize. Then oligomycin (2,5 µM) was added to identify the ADP-independent respiration. To measure the maximum ETC respiration, FCCP (1M) was added as a titration 1 µl at the time until no further increase in respiration could be detected. Rotenone (1mM) was added to inhibit the ETC and measure the oxygen consumption by other processes in the cells. A final addition of 5 µl succinate (cell permeable succinate prodrug) was performed to measure the succinate-dependent respiration.

2.5 Gene expression

2.5.1 RNA extraction

RNA was extracted from cell pellets using the MagMax™-96 Total RNA isolation kit (ThermoFisher Scientific, USA). To prevent degradation of RNA in the cell pellets, lysis/binding solution was added immediately after removal from -80 °C freezer. A guanidinium thiocyanate-based lysis buffer is used in the kit, to disrupt the cell membranes and inactivates nucleases. The samples were thawed at room temperature for 5 minutes, then the cell pellets were dispersed in lysis/binding solution by pipetting up and down. Magnetic beads that bind RNA, allowed contaminants to be removed in the presence of a magnet. DNA was removed by treating the nucleic acids with DNase. RNA was eluted from the beads in low salt elution buffer.

2.5.2 DNase treatment

An additional DNase treatment was employed to remove any further DNA contamination in the RNA sample. This was performed using the TURBO DNA-free™ Kit (ThermoFisher Scientific, USA). 5 µl TURBO DNase buffer, 1 µl TURBO DNase and 50 µl RNA sample were incubated for 30 minutes at 37 °C. Then 5 µl DNase Inactivation Reagent was added and after 5 minutes of incubation at room temperature, the tube was centrifuged for 2 minutes at 10 000 x g. The supernatant containing the RNA was added to a fresh tube and stored at -80 °C and used for all further RNA analyses.

2.5.3 RNA quantification and qualification

The yield of RNA from the cell pellets was quantified using Qubit® RNA HS Assay Kit (Invitrogen, USA). The kit contains a dye that bind specifically to RNA and emits fluorescence that can be measured by the Qubit Fluorometer (Invitrogen, USA). The manufacturer's protocol was followed, using 2 µl sample and 198 µl Qubit® working solution.

The quality of the RNA samples was assessed by gel electrophoresis on an agarose gel containing 2 % agarose (Invitrogen, USA) and 1x tris-acetate EDTA (TAE) buffer with 4µl/100ml PeqGreen (Peqlab, Germany). 1 µl Gel Loading Dye (New England BioLabs, USA) was added to 5 µl of RNA, and 5 µl of the mix was applied to the gel. In the first well

4 µl of 1kb ladder (Solis Biodyne, Estonia) was applied and the gel electrophoresis was run at 80 V and 400 mA for 40 minutes. Only samples with low degree of degradation were used for further analyses.

2.5.4 cDNA synthesis

cDNA was synthesized from the DNase treated RNA sample using the FIREScript RT cDNA Synthesis Mix (Solis BioDyne, Estonia). The reaction mix contained 1x RT Reaction Premix with Random Primers, 1,5 µl FIREScript Enzyme mix, 15,5 µl nuclease free water and 1 µl template RNA, to the total volume of 20 µl. The synthesis was performed on the 2720 Thermal Cycler (Applied Biosystems, USA) with primer annealing at 25 °C for 5 minutes, reverse transcription at 50 °C for 30 minutes and enzyme inactivation at 85 °C for 5 minutes.

2.5.5 qPCR

The gene expression of selected genes was measured using qPCR. Information about the primers used to target each gene is listed in table 2.1. The GOIs are either encoding proteins involved in the functions of mitochondria or the repair of DNA.

Table 2.1 Primer pairs used to measure gene expression with qPCR.

Target gene	Forward sequence (5' - 3')	Reverse sequence (5' - 3')
<i>GAPDH</i> (reference gene)	CCACATCGCTCAGACACCAT	GCGCCCAATACGACCAAAT
<i>NDUFA9</i>	ATTCCCCTTGCCGCTTTTTG	ATGTGCATCCGCTCCACTTT
<i>SDHB</i>	GCAGCAGTATCTGCAGTCCA	CGTAGAGCCCGTCCAGTTTC
<i>MT-ND2</i>	GCCCTAGAAATAAACATGCTA	GGGCTATTCTAGTTTTATT
<i>MT-ND6</i>	CAACCAGTAACTACTACTAA	ACTTTAATAGTGTAGGAAGC
<i>CYCS</i>	CATGGCCCCTCCCATCTACA	ATCTTGAGCCCCATGCGTTT
<i>NEIL1</i>	GCTGACCCTGAGCCAGAAGAT	CCCCAACTGGACCACTTCCT
<i>NEIL2</i>	ACCTGTGACATCCTGTCTGAGA AGT	TAATGATGTTCCCTAGCCCTGAG A
<i>OGG1</i>	CGAGCCATCCTGGAAGAACAG	ACATATGGACATCCACGGGCAC

To evaluate the amplification efficiencies of each primer pair, a two-fold serial dilution of cDNA was prepared, starting at 1:5 dilution. The other cDNA samples were diluted 1:5.

cDNA was added to a master mix containing HOT FIREPol® EvaGreen® qPCR supermix (Solis Biodyne, Estonia), forward and reverse primer. The reaction mix was run on CFX96 Touch™ Real-Time PCR Detection System (Bio-Rad, USA), starting with 95 °C for 15 min, followed by 40 cycles of 94 °C for 10 sec and 60 °C for 60 sec. At the end of the program, a melting curve was added, starting at 95 °C for 15 sec and then moving from 60 °C to 94 °C by an increase of 0,5 °C/cycle.

2.6 RNA-sequencing

From the non-degraded RNA samples with corresponding respiration data 21 samples were chosen for RNA sequencing. Duplicate libraries were prepared from two of the samples and a negative control was included. 127 ng of each library was pooled together and sequenced by Norwegian Sequencing Centre (Oslo) using the Illumina NovaSeq 6000 instrument.

2.6.1 Library preparation

To remove rRNA from the samples, the NEBNext® rRNA Depletion Kit NEB #E6350L (New England Biolabs, USA) was used. The effect of the rRNA depletion was evaluated by running qPCR with 18S primers and GAPDH primers before and after depletion. The 18S qPCR was performed by adding cDNA to a master mix containing HOT FIREPol® EvaGreen® qPCR supermix (Solis Biodyne, Estonia), forward and reverse primer. The reaction mix was run on CFX96 Touch™ Real-Time PCR Detection System (Bio-Rad, USA), starting with 95 °C for 15 min, followed by 40 cycles of 95 °C for 30 sec, 59 °C for 30 sec and 72 °C for 45 sec. The GAPDH qPCR was performed as described above (chapter 2.5.5).

Library preparation was performed with NEBNext® Ultra™ II RNA Library Prep Kit for Illumina® NEB #E7775S (New England Biolabs, USA). The kit instruction manual was followed, with some minor exceptions. The 2720 Thermal Cycler (Applied Biosystems, USA) were used for the majority of incubations, but the instrument only permitted a lid temperature of 103 °C. For incubations at temperatures ≤ 37 °C a heating block was used.

The amount of input RNA was approximately 400 ng and 9 cycles were used in the PCR enrichment step.

2.6.2 Library normalization and validation

The individual RNA-seq libraries were quantified using qubit. Then equimolar concentrations of the libraries were pooled together to obtain approximately the same sequencing depth for all samples. The pooled library was also quantified using qubit, but a more accurate quantification was performed by Norwegian Sequencing Centre to ensure optimal density of clusters on the flow cell. An assessment of the distribution of fragment lengths was done by gel electrophoresis to ensure a majority of fragments with sizes that give efficient amplification on the flow cell (Bronner et al., 2014). The gel was prepared as described in chapter 2.5.3 and the samples were run at 90 V and 400 mA for 45 minutes.

2.7 In vivo concentrations of branched chain fatty acids

The luminal SCFA concentrations have been determined by others, by autopsy and by measuring in fecal samples (Cummings et al., 1987; Norin et al., 2004; Topping & Clifton, 2001). On the other hand, there is not much information about BCFA concentrations (Taormina et al., 2020). Based on the estimated intake of BCFA, the luminal concentrations were assumed to be in the μM order of magnitude (Dingess et al., 2017; Ran-Ressler et al., 2013). To verify this assumption, the BCFA concentrations were measured in fecal samples, provided by the preventADALL study. The study is registered at clinicaltrials.gov with the identifier NCT02449850 and is approved by the Regional Ethical Committees for Medical and Health Research Ethics (REK) in South-Eastern Norway (2014/518) and the Regional Ethical Trial Committee of Stockholm (2015/4:3).

Samples from infants aged 12 months were retrieved from the PreventADALL biobank. The fecal samples were thawed on ice and approximately 50 mg of each sample were weighed accurately into gas chromatography (GC) vials. Further sample preparation and GC analysis was performed by Vitas AS (Oslo).

2.8 Data analysis

2.8.1 Relative quantification of qPCR gene expression

The real-time qPCR data was analyzed using the software Bio-Rad CFX Maestro 1.1, version 4.1.2433.1219 (Bio-Rad, USA) and the gene expression of the GOIs in the groups of fatty acid-treated samples relative to the control group was calculated using the $2^{-\Delta\Delta C_t}$ method (Livak & Schmittgen, 2001). This will hereafter be referred to as the $2^{-\Delta\Delta C_q}$ method.

Equation 1 was employed to normalize the C_q values of GOIs to the value of the reference gene within the same sample. This was done to correct for the variation in C_q values that was not related to the expression level, but rather the difference in cDNA concentration.

$$\Delta C_q = C_{q, \text{gene of interest}} - C_{q, \text{reference gene}} \quad (1)$$

The ΔC_q values were averaged within each treatment group and normalized to the average of the untreated control samples using equation 2.

$$\Delta\Delta C_q = \overline{\Delta C_{q, \text{treatment}}} - \overline{\Delta C_{q, \text{control}}} \quad (2)$$

The resulting $\Delta\Delta C_q$ value reflected the difference in PCR cycles between the given treatment and control for each GOI. As the C_q is inversely proportional to the log transcript number, the relative change in gene expression was obtained by transforming to $2^{-\Delta\Delta C_q}$.

2.8.2 Gene expression using RNA-sequencing

The RNA-seq data was analyzed using the CLC Genomics Workbench 20.0.4. (QIAGEN, Denmark) software. The reads were trimmed based on quality and adapters were removed by automatic read-through trimming. Default parameters of match score = 1, mismatch cost = 2, gap cost = 3 and maximum number of hits for read = 10 were used to map the reads to the human reference genome (GRCh38). The mapping tool handled multimapping reads with the Expectation Maximization (EM) estimation algorithm and calculated the gene expression levels as Transcripts per Million (TPM) as shown in equation 3 (Wagner et al., 2012).

$$TPM = \frac{\text{number of transcript reads} * \text{mean read length}}{\text{total number of transcripts (millions)} * \text{transcript length}} \quad (3)$$

TPM is an alternative to the previously popular Reads Per Kilobase of transcript per Million (RPKM). TPM considers the length of the transcript, correcting for the differences in number of reads between long and short transcripts, that does not depend on expression level. It also corrects for variations in library size or sequencing depth by including the total number of unique transcripts detected in the sample. Even though the TPMs are calculated for each sample individually, this method is more appropriate for comparing expression levels between samples than RPKM. This is because the sum of TPMs is the same in each sample while the sum of RPKMs varies between samples.

The variation in expression patterns of the samples were visualized using the PCA for RNA-Seq tool. The CLC Genomics Workbench tool Differential Expression for RNA-Seq was used to reveal genes with significant difference in expression between treated and untreated samples.

These tools employed a different normalization approach. The read counts are assumed to follow the negative binomial distribution and Trimmed Mean of M values (TMM) normalization was used (QIAGEN, 2020). This normalization method assumes that most genes are not differentially expressed (DE) to calculate effective library sizes that allow comparison of samples with different sequencing depths (Robinson & Oshlack, 2010). Counts per million mapped reads (CPM) values of expression levels were calculated as shown in equation 4.

$$CPM = \frac{\text{number of transcript reads}}{\text{total number of reads in sample (millions)}} \quad (4)$$

The CPM formula does not normalize for transcript length, but this is irrelevant as it is used to compare the same transcript between samples. Gaussian cross-sample normalization was finally performed to give a distribution where the mean is zero and the standard deviation is one.

2.8.3 Pathway analysis

Gene symbols corresponding to the RefSeq IDs of the significant DE transcript variants were retrieved with the g:Profiler g:Convert tool (Raudvere et al., 2019). The lists of DE genes for each treatment were then submitted to the Reactome Analysis Data webtool. Reactome performs an over-representation analysis, to determine if the gene list contains more components of a particular pathway in the database than is expected by chance (Fabregat et al., 2017).

2.8.4 Statistical analysis

T-test

The statistical significance of gene expression measured by qPCR was determined with a two-sample T-test in Microsoft Excel. The test was performed with ΔC_q values for the samples with each treatment against the controls. These values are normally distributed, and the test was used to determine if the mean within each treatment were equal to the mean of the controls. A 5% significance level was used.

Principal component analysis (PCA)

Normalized log CPM values for all samples were z-score normalized to distribute the expression levels for each gene around zero and used in a principle component analysis (PCA). This method is based on the positioning of samples in a multidimensional space spanned by all the detected genes. The PCA reduces the dimensionality of the data into principal components that explain most of the variation between the samples (Wold, 1987). These principal components were used to assess if the variation in gene expression between samples could be explained by some of the fatty acid treatments.

Differential gene expression

The Differential Expression for RNA-Seq tool fit a Generalized Linear Model (GLM) to the normalized log CPM data. The statistical significance was assessed by a Wald test that determines if the treatment coefficient in the model are non-zero (QIAGEN, 2020).

Multiple hypothesis testing

The probability scores of the differential expression and pathway analyses were false discovery rate (FDR) corrected for multiple hypothesis testing by the Benjamini-Hochberg procedure. The p-value of a single hypothesis test is the probability that the null hypothesis is falsely rejected, a so-called type I error (Banerjee et al., 2009). When multiple hypotheses are tested at once, there is an increasing probability that this error occurs. The Benjamini-Hochberg procedure therefore calculates FDR-adjusted p-values, which are more strict (Benjamini & Hochberg, 1995). The significance level of the adjusted p-values was set to 5%.

Correlation analysis

The quality of the RNA-seq analysis was assessed using a Pearson correlation analysis. This was performed by a pairwise plotting of TPM values between the untreated biological replicates. The same method was used to compare the GOI expression levels from qPCR and RNA-seq. The samples TPM values were plotted against ΔC_q for each gene.

3 Results

3.1 Establishment of in vitro system

To characterize the growth and respiration of the cell model, $3,0 \cdot 10^5$ cells were added to 12 plates and grown for up to 6 days. Every 24 hours, the cells were harvested from two plates to count the number of cells. Figure 3.1 shows the estimates of the total cell numbers on each plate, as well as a graph showing the average of each time point.

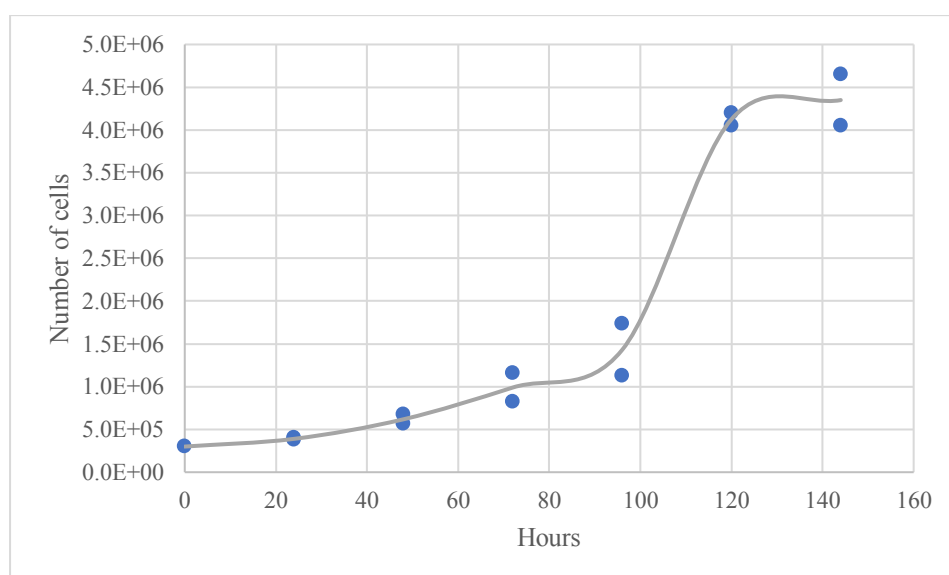


Figure 3.1 Number of Caco-2 cells on plates after different growth durations. Each plate had a diameter of 10 cm and contained $3,0 \cdot 10^5$ cells at 0 hours. The blue dots represent the cell number estimates and the number of hours of incubation for each plate, with two parallels grown for the same time. The grey line shows the average estimates at each time point.

The cells showed a slow growth rate the first 96 hours, when the cell density on the plate was low. Then the cell numbers increased rapidly from approximately 1,5 million to above 4 million between 96 and 120 hours. After 120 hours the growth rate decreased, and the cell number reached a maximum of about 4,5 million cells.

Bioenergetic profiling was performed on the cell cultures every 24 hours, starting 48 hours after plating. Only one parallel was measured at 72 hours. Figure 3.2 shows four different respiratory states of the samples at the five time points of measurement.

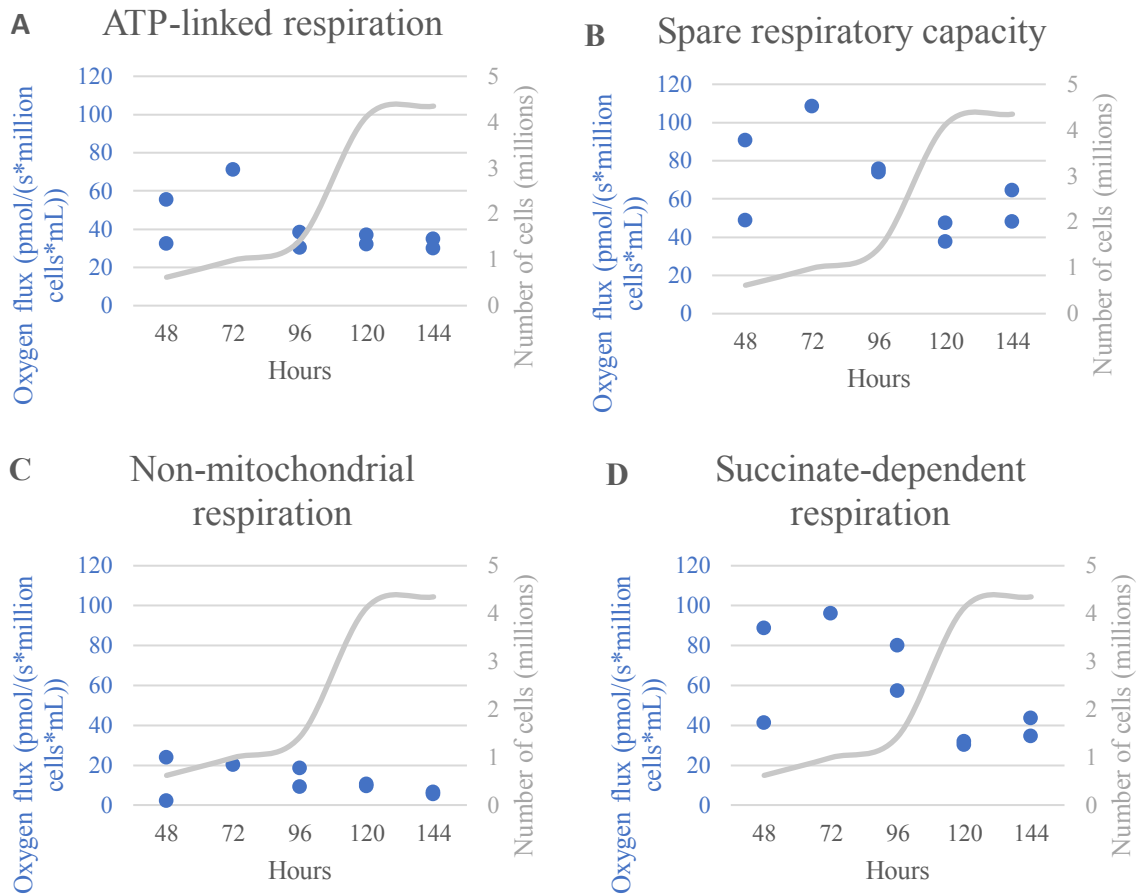


Figure 3.2 Respirometry measurements for the cell cultures at different durations of growth. The panels show the levels of oxygen flux related to ATP-linked respiration (A), spare respiratory capacity (B), non-mitochondrial respiration (C) and succinate-dependent respiration (D). The blue dots show the oxygen flux for each sample, while the grey line represent the average number of cells in the samples, at the given time.

At the first three time points (48-96 hours), the succinate-dependent respiration, ATP-linked respiration and spare respiratory capacity was higher than at the last two time points (120 and 144 hours). There was also more variation between the parallels, as well as between each time point at lower cell density.

The characterization was done to find the best time/cell number to analyze cell cultures.

Based on these results, it was decided to analyze the cell cultures shortly after reaching a cell number of approximately 4 million.

3.2 Gene expression using RNA-seq

From the extracted RNA samples with corresponding respiration measurements, a subset was prepared for RNA-seq. The samples were selected depending on RNA quality, assessed by

gel electrophoresis and the gel pictures are presented in appendix A. The prepared libraries were pooled and sequenced on the Illumina NovaSeq 6000 system by Norwegian Sequencing Centre (Oslo). Using the CLC Genomics Workbench software, the reads were mapped to the human reference genome (GRCh38) and gene expression was calculated as log CPM values. Figure 3.3 shows a plot of the PCA based on the gene expression levels of all sequenced samples.

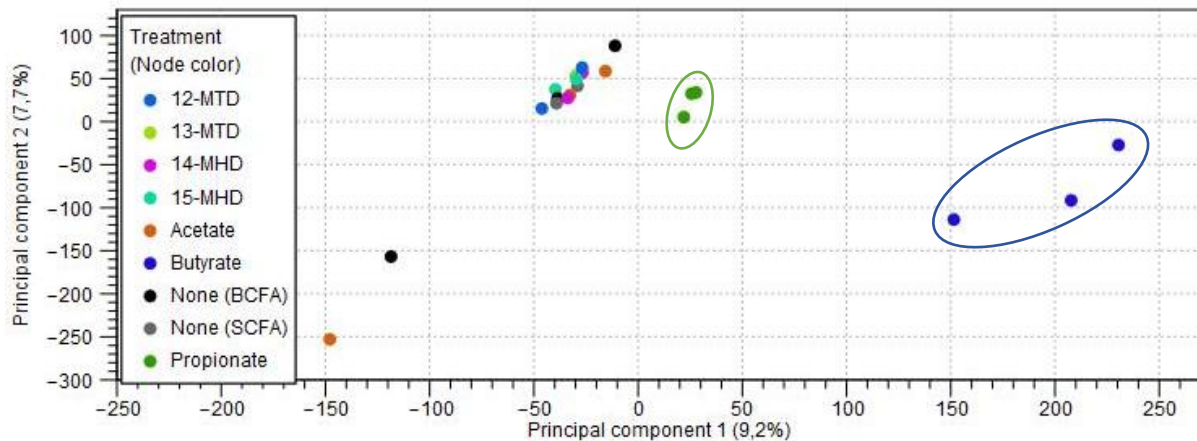


Figure 3.3 PCA plot based on gene expression of treated samples and controls. From PCA for RNA-Seq tool in CLC Genomics Workbench. The propionate-treated samples are marked with a green circle and the butyrate-treated samples are marked with a blue circle. The percentage of the variation explained by each principal component is stated in the axis titles.

The plot shows that the butyrate-treated samples are separated from the rest. The propionate-treated samples are also grouped together. They are closest to the majority of the samples but move towards the butyrate-treated along the first principal component. Principal component 1 explains 9,2 % of the variation and is the component that separates the propionate-treated and butyrate-treated samples from the rest.

Differentially expressed transcript variants

The genes were tested for differential expression between the treatments and controls. The BCFA-treated cells revealed 1 DE transcript variants for 12-MTD, 2 for 13-MTD and 1 for 14-MHD. Figure 3.4 shows a Venn diagram of the DE transcript variants for the SCFA-treatments. The complete list of DE transcript variants for all treatments can be found in appendix D. For the butyrate-treated cells, 202 variants were up-regulated and 141 down-regulated. For the propionate-treated cells 12 variants were up-regulated and 7 down-regulated. For acetate-treated cells 2 transcripts were up-regulated and 2 were down-regulated.

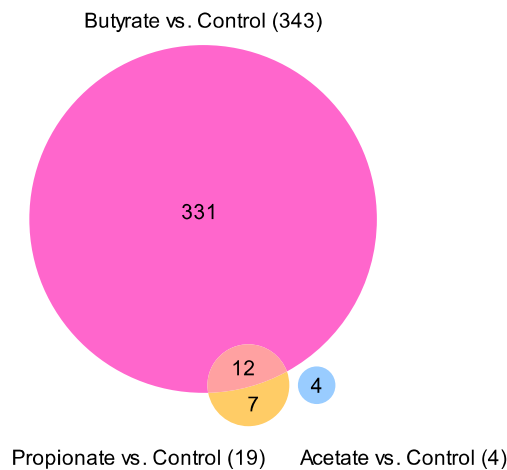


Figure 3.4 Venn diagram of DE transcript variants between SCFA-treated cells and controls. Each circle represents the number of DE variants with the given treatment, compared to control samples. The total number is indicated in parenthesis, while the exclusive and shared numbers are inside the circles. The figure is generated by the Create Venn Diagram tool in CLC Genomics Workbench.

The Venn diagram shows a decreasing number of DE transcript variants for cells treated with butyrate, propionate and acetate respectively. The number of DE transcript variants with butyrate-treatment exceeds by far the other treatments and the majority of DE variants for propionate-treated cells are shared with the butyrate-treated cells.

Pathways associated with the differentially expressed genes

The RefSeq IDs of the DE transcript variants were translated to gene names with the g:Convert tool. Not all IDs could be assigned, and some were variants of the same gene. This resulted in 308 genes for the butyrate-treated cells and 18 genes for propionate-treated samples. The lists of differentially expressed genes-were tested for pathway overrepresentation using the Reactome Analysis Data webtool. 99 identifiers for butyrate-treatment and 1 for propionate-treatment could not be found in any of the pathways in the database. 59 significant pathways were identified for butyrate-treatment, but none for propionate-treatment. The chosen significance level was FDR-adjusted p-value < 0,05. Table 3.1 shows the pathways for butyrate-treated cells. The top 20 pathways for propionate-treatment is presented in appendix E.

Table 3.1 Pathways with significant (FDR-adjusted p-value < 0,05) overrepresentation of differentially expressed genes in butyrate-treated cells. The pathways were identified using the Reactome Analysis Data webtool.

PATHWAY NAME	ENTITIES FDR
Prefoldin mediated transfer of substrate to CCT/TriC	1,84E-04
Cooperation of Prefoldin and TriC/CCT in actin and tubulin folding	5,90E-04
Cellular responses to external stimuli	5,90E-04
Formation of tubulin folding intermediates by CCT/TriC	5,90E-04
Cellular responses to stress	5,90E-04
RHO GTPases activate IQGAPs	1,49E-03
Selective autophagy	1,49E-03
Recycling pathway of L1	3,89E-03
Apoptosis induced DNA fragmentation	4,37E-03
Microtubule-dependent trafficking of connexons from Golgi to the plasma membrane	4,37E-03
Nuclear Envelope (NE) Reassembly	4,37E-03
Transport of connexons to the plasma membrane	4,66E-03
Aggrephagy	4,68E-03
Attenuation phase	4,68E-03
Post-chaperonin tubulin folding pathway	5,88E-03
Gap junction trafficking	7,60E-03
Mitotic G1 phase and G1/S transition	7,60E-03
Formation of Senescence-Associated Heterochromatin Foci (SAHF)	7,60E-03
Chaperonin-mediated protein folding	7,60E-03
Signal regulatory protein family interactions	8,98E-03
RUNX3 regulates WNT signaling	9,85E-03
Gap junction trafficking and regulation	9,85E-03
Hedgehog 'off' state	9,85E-03
Protein folding	9,85E-03
HSF1-dependent transactivation	1,23E-02
RHO GTPases Activate Formins	1,35E-02
G1/S Transition	1,37E-02
Regulation of HSF1-mediated heat shock response	1,46E-02
Post NMDA receptor activation events	1,47E-02
Activation of AMPK downstream of NMDARs	1,47E-02
Interleukin-4 and Interleukin-13 signaling	1,47E-02
HSP90 chaperone cycle for steroid hormone receptors (SHR)	1,55E-02
Insulin-like Growth Factor-2 mRNA Binding Proteins (IGF2BPs/IMPs/VICKZs) bind RNA	1,69E-02
The role of GTSE1 in G2/M progression after G2 checkpoint	1,86E-02
Cell Cycle, Mitotic	1,86E-02
TFAP2 (AP-2) family regulates transcription of cell cycle factors	1,86E-02
Transcriptional activation of p53 responsive genes	1,86E-02

Transcriptional activation of cell cycle inhibitor p21	1,86E-02
Mitotic Anaphase	1,93E-02
Mitotic Metaphase and Anaphase	1,95E-02
Sealing of the nuclear envelope (NE) by ESCRT-III	2,19E-02
Signaling by Hedgehog	2,50E-02
FOXO-mediated transcription of cell cycle genes	2,53E-02
Intraflagellar transport	2,60E-02
Gap junction assembly	2,60E-02
Macroautophagy	2,60E-02
FOXO-mediated transcription	2,61E-02
Cell Cycle	2,99E-02
HSF1 activation	3,04E-02
Estrogen-dependent nuclear events downstream of ESR-membrane signaling	3,05E-02
Activation of NMDA receptors and postsynaptic events	3,09E-02
RUNX3 regulates CDKN1A transcription	3,11E-02
Cellular response to heat stress	3,11E-02
Translocation of SLC2A4 (GLUT4) to the plasma membrane	3,59E-02
COPI-independent Golgi-to-ER retrograde traffic	4,11E-02
EML4 and NUDC in mitotic spindle formation	4,29E-02
TP53 Regulates Transcription of Genes Involved in G1 Cell Cycle Arrest	4,66E-02
Autophagy	4,66E-02
Assembly and cell surface presentation of NMDA receptors	4,75E-02

The butyrate-treated cells had differentially expressed genes related to pathways for a range of different cellular functions, such as regulation of cell cycle, signaling and stress response. Although none of the identified pathways in cells with propionate-treatment were significant, some of the top pathways could be found among the significant pathways in butyrate-treated cells.

3.3 Gene expression by qPCR

A set of primers for eight GOIs and a reference gene (*GAPDH*) was selected to assess the function of the mitochondria with the different treatments. Due to technical difficulties with respirometry measurements, the experiment had to be repeated for SCFA treatments. This resulted in more replicates that could be analyzed by qPCR. The number of replicates were less than three for the BCFA treatments because the RNA quality was too poor in some of the samples to be analyzed with qPCR or RNA-seq. Gene expression measured with qPCR, estimated using the $2^{-\Delta\Delta Cq}$ method is presented in figure 3.5. A $2^{-\Delta\Delta Cq}$ value of 1 is equivalent

to the mean expression level of control samples. The statistical significance between treated and un-treated samples for each gene was assessed using two-sample t-test on the ΔC_q values.

Because this method depends on equal amplification between each GOI and the reference gene, the amplification efficiencies were determined using a 2-fold dilution series of cDNA. The efficiencies of each primer pair in the two experiment rounds are presented in appendix B, together with R^2 values of the plotted C_q of the dilutions.

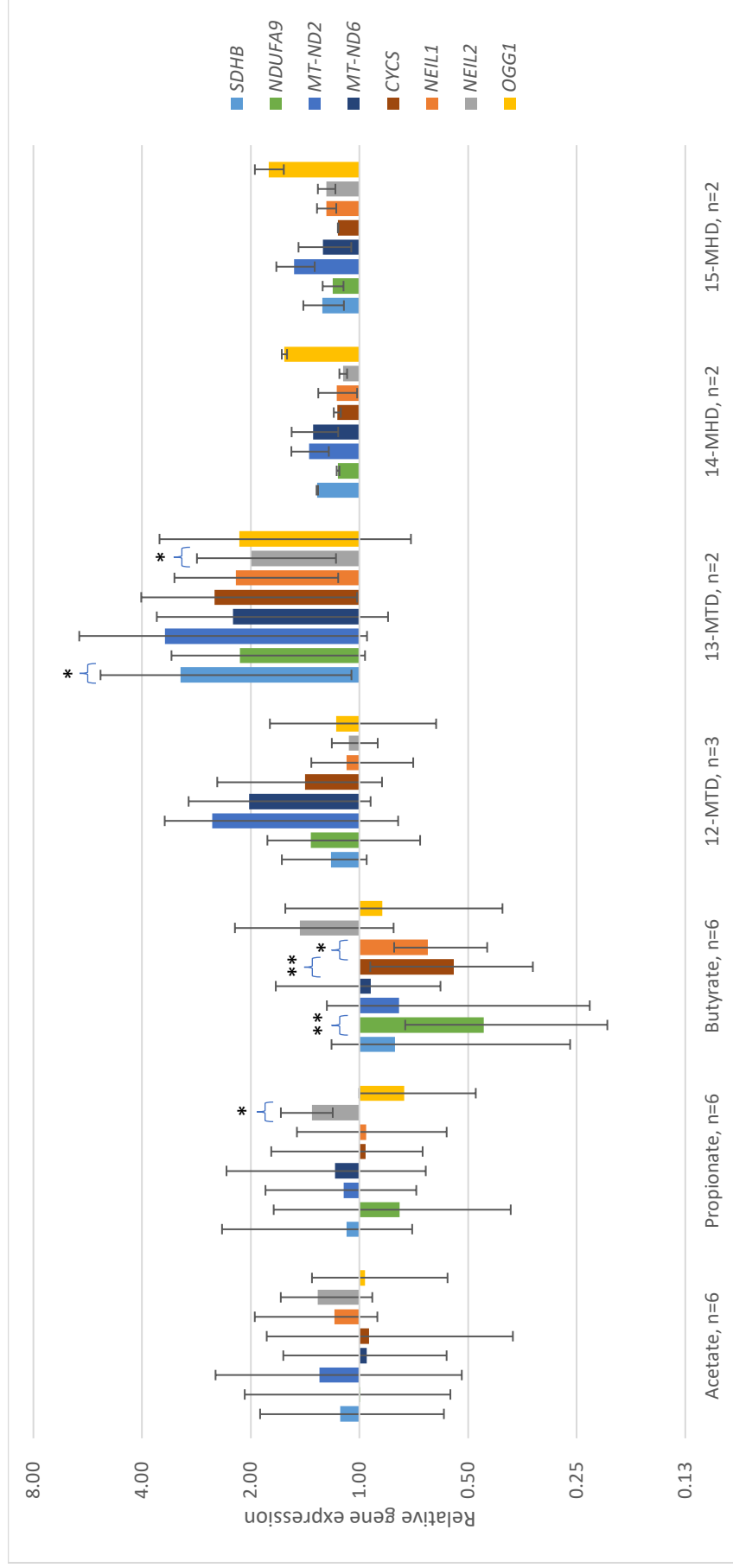


Figure 3.5 Average expression levels of treated Caco-2 cell samples relative to controls with the $2^{-\Delta\Delta Ct}$ method for genes in after treatment with three SCFA and four BCFAs. The number of replicates (n) with each treatment is indicated on the x-axis. The treatments were compared to n=5 control samples. Error bars show maximum and minimum values within each treatment. * $p < 0.05$, ** $p < 0.01$.

Propionate-treatment lead to a significant up-regulation of *NEIL2*. Cells treated with butyrate showed a significant down-regulation of *NDUFA9*, *CYCS* and *NEIL1*. For the BCFA, only 13-MTD lead to a significant change: *NEIL2* and *SDHB* were both up-regulated. However, this was based on two replicates with large variation. Although the regulation was not significant for 14-MHD or 15-MHD, both of these BCFA had very similar replicates that indicated some up-regulation for all genes.

The qPCR results were compared with RNA-seq results by mapping reads to the full sequences of the GOIs. Correlations between qPCR and RNA-seq were assessed by the R^2 -value of a plot between log TPM and log $2^{-\Delta\Delta Cq}$ values. The correlation between *GAPDH*-normalized qPCR results and RNA-seq results gave a R^2 of 0,88. Scatter plots of all TPM-values between control-samples gave R^2 -values between 0,46 and 0,60. All R^2 -values are shown in appendix C.

3.4 Respiration

Bioenergetic profiling by respirometry was done on the cell cultures after a 24-hour treatment period. The measurements were normalized by the number of cells in each sample. The estimated levels of ATP-linked respiration, spare respiratory capacity, non-mitochondrial respiration and succinate-dependent respiration are presented in figure 3.6 for three replicates of each treatment. One group of control samples was only added dH₂O and analyzed together with the SCFA-treated samples, while the other group was added DMSO and analyzed with the BCFA-treated samples. The results were assessed with a two-sample t-test, but none of the treatments were significantly different from the controls.

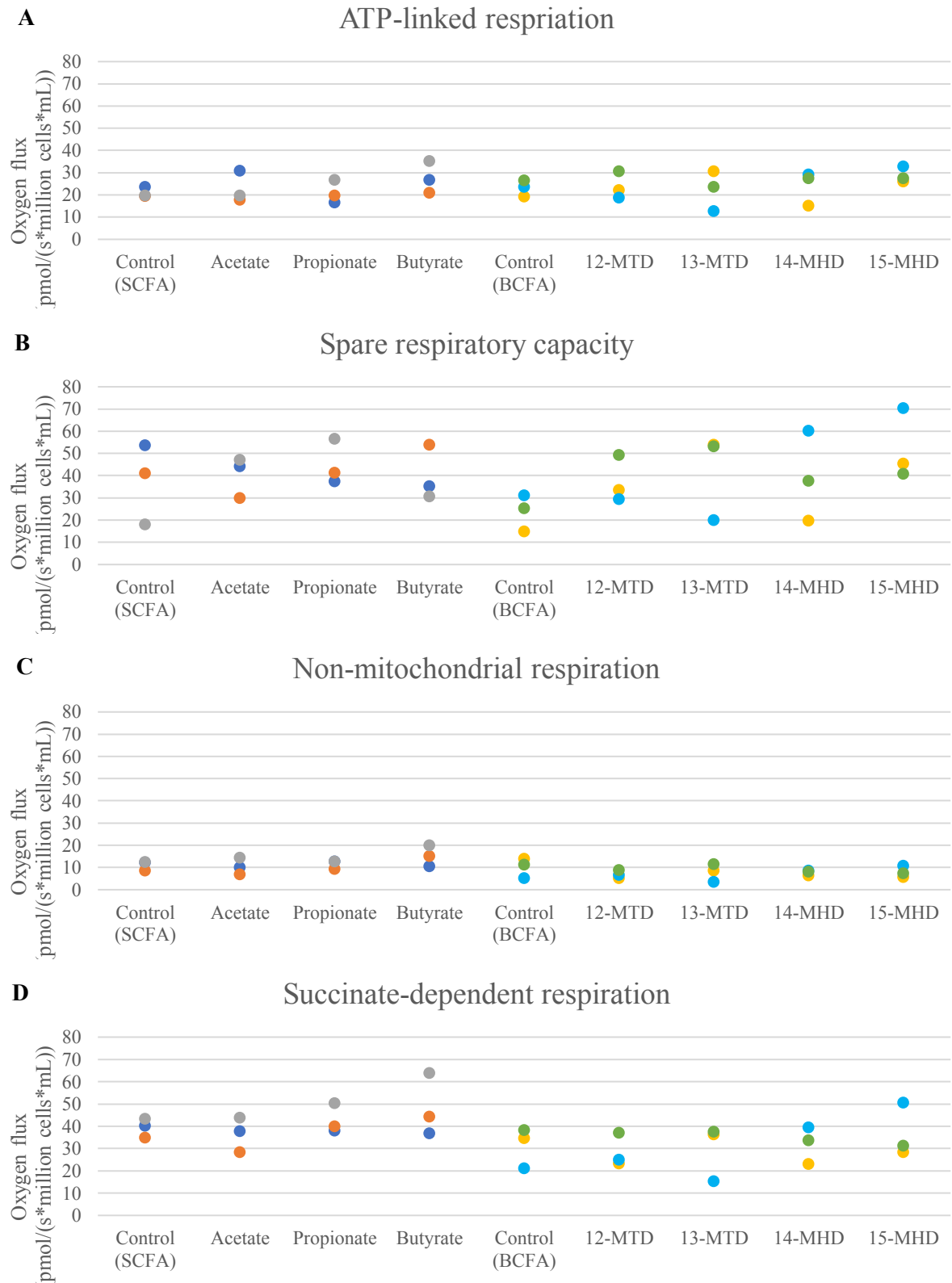


Figure 3.6 Respiration of untreated cells and cells treated with SCFA or BCFA, measured with Oxygraph-2K. The panels show the levels of oxygen flux related to ATP-linked respiration (A), spare respiratory capacity (B), non-mitochondrial respiration (C) and succinate-dependent respiration (D). The colors of the dots indicate which samples were analyzed on the same day.

Butyrate-treatment led to slightly higher average oxygen consumption linked to ATP-production and higher succinate-dependent respiration. All of the BCFA, in particular 15-MHD showed increased spare respiratory capacity compared to the corresponding group of control samples.

3.5 Verification of BCFA concentrations

BCFA concentrations were measured by GC in 174 of the fecal samples from infants at 12 months of age. Two samples were lost during the preparation and could not be measured. The limit of quantification (LOQ) was 0,005 mg fatty acid/g feces. Table 3.2 shows the median concentration, as well as the 2,5 % and 97,5 % quantiles of the four BCFA of interest in this study. The molar concentration was calculated based on a fecal density of 1,06 g/ml (Penn et al., 2018). The median and quantiles of all the detected fatty acids in the samples can be found in appendix F.

Table 3.2 Median and quantiles for in vivo concentrations (μM) of the fatty acids of interest in 174 samples from infants in the PreventADALL cohort. The concentrations were determined by GC, performed by Vitas (Oslo).

FATTY ACID	MEDIAN	2,5 % QUANTILE	97,5 % QUANTILE
12-MTD	540,5	67,8	2093,3
13-MTD	176,2	39,4	619,2
14-MHD	65,0	23,5	354,6
15-MHD	96,0	36,1	375,0

The four BCFA that were used as a treatment in this study, were present in the fecal samples at median concentrations from 65,0 to 540,5 μM . 12-MTD was most abundant in the samples of the four, and 14-MHD the least abundant.

4 Discussion

4.1 Differentially expressed genes and associated pathways with fatty acid treatments

4.1.1 Effect on gene expression by butyrate and propionate

The large number of DE genes by butyrate-treatment (figure 3.4) supports that this fatty acid is not only important as a source of energy, but also have the power to impact other processes in the cell. Acetate is the second most activated SCFA by the colonocytes (Roediger, 1982), but the number of DE genes is higher with propionate-treatment. An overlap between DE genes induced by butyrate and propionate points toward these fatty acids inducing some of the same mechanisms in the cells. This may be due to the ability of SCFAs to inhibit HDACs (Boffa et al., 1978). Butyrate is the most potent inhibitor, while propionate has shown more moderate effects (Hinnebusch et al., 2002). This would also explain why butyrate shows greater effect on gene expression than other fatty acids. At the pathway level, there is also an overlap between butyrate- and propionate-treated cells. The number of DE genes with propionate-treatment was too low to get significant results in pathway analysis (appendix E, table E.1) but the most significant pathways by butyrate-treatment include some of the DE genes shared with propionate (table 3.1) Together, these results suggest that propionate may be of importance in infants, before they are colonized by butyrate producing bacteria.

4.1.2 Impact on the cell cycle regulation by butyrate-treatment

The pathways significantly influenced by butyrate-treatment are associated with different cell functions. Some of them are regulation of cell cycle and signal transduction. The influence by butyrate on cell cycle regulation has also been observed by others (Archer et al., 1998; Litvak et al., 1998). The pathway analysis shows that butyrate inhibits the transition between G1 and S phases of the mitosis. This is characterized by the observed up-regulation of *CDKN1A* and *CCN1*, and down-regulation of *MYC* and *CCND* genes. AMPK activation and suppression of Wnt signaling are both potential contributors to this effect, but it might also be a result of cross-talk between the mechanisms, as AMPK has been shown to suppress Wnt signaling (Park et al., 2019). Butyrate has been shown to activate AMPK in Caco-2 cells (Peng et al., 2009), which promotes cell cycle arrest by inducing p53 transcription factor which target *CDKN1A* (p21) (Kim et al., 2016). AMPK is an energy sensor that is activated when the

levels of ATP in the cell is low to suppress anabolism and increase catabolism (Carling, 2004). However, the activation can also be induced to promote apoptosis without energy depletion (Patel et al., 2015). This makes AMPK important in the regulation of autophagy (Kim et al., 2016).

The suppression of Wnt signaling inhibits transcription of *CCND1* and *MYC*, which in turn lead to up-regulation of p21(*CDKN1A*) (Pinto et al., 2003). *MYC* is an oncogene and overactive Wnt signaling have been shown to up-regulate this gene in colorectal cancer (Rennoll & Yochum, 2015). Activity of Wnt is required for cell differentiation and induce mitochondrial biogenesis (Fu et al., 2019; Noah et al., 2011). Both aspects are important in the development of new colonocytes from stem cells but would hinder the renewal of the epithelium if active in mature colonocytes. Suppression of Wnt signaling by butyrate may therefore be an important function to maintain the epithelial homeostasis.

The pathway analysis provides only a limited insight into the cellular processes, and exactly how the pathways are influenced by butyrate is still not clear. However, the gene expression patterns point towards butyrate inducing cell cycle arrest in the Caco-2 cells, which could be part of its anti-cancer effect. If the fatty acid lead to a similar expression patterns in healthy colonocytes, this supports the hypothesis that butyrate is involved in the epithelial homeostasis.

4.1.3 Activation of cellular responses to stress

Another function associated with the DE genes is cellular stress response. Some of the genes involved in this are tubulin genes, which are up-regulated with both butyrate-and propionate-treatment. Tubulin expression is subject to autoregulation where unassembled subunits lead to less stable mRNA and therefore less translation of tubulin polypeptides (Gay et al., 1989). The tubulin mRNA is therefore not degraded when the tubulin heterodimers are stabilized through acetylation. The ability of butyrate to inhibit HDAC has mostly been associated with gene activation through histone acetylation. However, HDAC can also deacetylate non-histone proteins, such as P53 and JUN transcription factors, as well as tubulin (Zhang et al., 2003). Donohoe et al. (2012) show that tubulin can be acetylated by butyrate. The increased levels of tubulin-mRNA with butyrate-treatment is probably due to decreased degradation of mRNA, and not higher levels of transcription.

Together with other DE genes, the tubulin genes are involved in pathways associated with protein folding, aggrephagy, signal transduction and gap junction trafficking. Tubulin proteins are the constituents of microtubules, which have several functions in the cell. Microtubules make up the cytoskeleton in the cell, the mitotic spindles in mitosis and they also mediate the transport of proteins and organelles that is required in stress response (Parker et al., 2014). Microtubule associated proteins (MAPs) that increase the stability of microtubules (Cooper, 2000) are also up-regulated with butyrate-treatment in this study. As the cells show signs of cell cycle arrest, the increased tubulins levels are most likely a sign of activation of the cells stress response system. Heat shock proteins (HSP) is a group of proteins involved in the response to different types of stress, such as oxidative stress (Kurashova et al., 2019). Genes encoding HSP70 were up-regulated by butyrate. This protein has previously been found to inhibit the pro-inflammatory cytokine IL-8 in Caco-2 cells (Malago et al., 2005). This could therefore be part of the mechanism behind the anti-inflammatory properties of butyrate that are important for the colonic health.

4.2 The influence on mitochondrial activity by fatty acids

4.2.1 A shift in respiration with butyrate-treatment

All three SCFAs can be utilized as sources of energy by colonocytes (Clausen & Mortensen, 1995). The increase in ATP-linked respiration by butyrate-treated cells (figure 3.6) seems contradictory to the down-regulation of ETC genes (figure 3.5) in the same cells. However, the increase in succinate-dependent respiration points towards a shift in the mitochondrial activity towards β -oxidation. This would also explain lower expression of components in complex I, as this part of the ETC would be less active. The oxidation of fatty acids leads to a higher oxygen consumption per molecule of ATP produced, which entails a higher ROS production (Litvak et al., 2018). These compounds cause oxidative damage of the DNA, but also functions as signal molecules involved in regulation of metabolism and cell proliferation (Zhang et al., 2016). A sign of the increased ROS production in these samples is the up-regulation of *NEIL2*, which is involved in transcription-coupled BER (Banerjee et al., 2011). Of the three investigated genes involved in DNA repair, this was the only one with increased expression. *NEIL1* is also a BER enzyme, but functions primarily in prereplicative repair during S-phase (Hegde et al., 2013). As butyrate inhibit the cells G1/S transition this might explain why the *NEIL1* gene was not up-regulated. The expression of DNA repair genes is

only an indication of the levels of DNA-damage and does not reveal how efficiently the damage is repaired. Further efforts should therefore be made to estimate the levels of DNA-damage.

Why butyrate-treatment lead to significant down-regulation of *CYCS* is not clear. When situated in the mitochondrial inner membrane, cytochrome c has the ability to eliminate O_2^- and H_2O_2 (Zhao et al., 2003)). Increased expression of cytochrome c precedes its release into the cytosol, which is associated with apoptosis (Liu et al., 1996; Sanchez-Alcazar et al., 2001). As butyrate is known to induce apoptosis, an up-regulation of *CYCS* would therefore rather be expected (Fung et al., 2012).

4.2.2 The effect on respiration by propionate-treatment

Propionate show some of the same effects on respiration as butyrate, but to a lesser extent. The slight increase in succinate-dependent respiration may indicate that this treatment also induces β -oxidation. These results suggest some increase in β -oxidation induced by propionate, but the unchanged expression of complex I genes indicate that the ATP-production in the cells still rely on the activity of the TCA cycle. As propionate is a precursor for glucose in gluconeogenesis, it would be interesting to see if the observed effects persist with lower concentrations of glucose in the medium, or if this would lead to more β -oxidation.

The increase in spare respiratory capacity by propionate-treatment was not observed in butyrate-treated cells. This property signifies increased abilities to overcome stress, such as oxidative stress (Hill et al., 2009). A mechanism to maintain the energy production during oxidative stress is mitochondrial biogenesis (Wenz, 2013). However, this would also be accompanied by up-regulation of ETC enzymes and no significant changes were observed in the gene expression of ETC complexes with this treatment. Another mechanism that can increase the spare respiratory capacity is the activation of antioxidant systems that eliminate ROS (Yamamoto et al., 2016). Similar to butyrate-treated samples, gene expression measurements show significant increase in *NEIL2* expression.

4.2.3 Indications of increased mitochondrial activity by BCFA-treatment

For the BCFA-treatments, less than three replicates could be included in the gene expression analysis for each treatment. The samples treated with 12-MTD and 13-MTD showed large variation in expression of GOI between the replicates. To determine if the observed changes in gene expression are significant, the experiments should be repeated with larger number of replicates. Within the 14-MHD and 15-MHD groups, the variation was lower. This strengthens the indication of up-regulation by the treatments, even though the observed effect was small. A higher treatment concentration could be used to determine if these fatty acids have a significant influence on the cells. The increased spare respiratory capacity together with the overall up-regulation of ETC-genes for the two 17-carbon fatty acids suggest that these may induce mitochondrial biogenesis. This could also explain the increase in ATP-linked respiration by 15-MHD-treatment but should be investigated further by estimating the number of mitochondria.

4.3 The use of Caco-2 cells as a colonocyte model

4.3.1 Respirometry measurements at different cell densities

In this study, Caco-2 cells were used as a model for the colonocytes in the gut epithelium. Previous research has shown that at confluence, these cells share characteristics with colonocytes (Engle et al., 1998). The continuous monolayer, formed by the cells at sufficient cell density, resembles the physiologic condition in the gut epithelium and treatments were absorbed from the apical side of the cell, which is the one facing the lumen. However, when the respiration was measured, the cells were had to be dispersed in the medium, rendering all cell surfaces exposed to the substrates. This may have led to higher oxygen consumption and an altered production of metabolites by the cells (Roediger, 1982).

At low cell density, the cells showed high levels of oxygen consumption and the respiration rate changed rapidly (figure 3.2). This could introduce a high level of background noise if the cells were analyzed in this phase. Reaching a sufficient cell density, the cells entered a phase where growth rate increased drastically (figure 3.1). Analyzing cells in this phase would make it difficult to obtain samples with similar number of cells. During the last phase, both the growth and the respiration stabilized. However, if the cells were left too long in this phase, they would begin to differentiate, which would lead to more heterogenous cells and less resemblance to colonocytes.

The aim was to analyze the cells in the narrow window between rapid growth and differentiation. The counting technique that was used depended on cells being separated from each other and dispersed evenly in the medium to give a reliable estimate. The cells were however difficult to disperse, which could have led to pairs or clusters of cells being counted as one. The method that was used to count the cells is also known to give a variable result (Cadena-Herrera et al., 2015). This may explain some of the observed variation in cell numbers and could have an impact on the accuracy of the respiration measurements, as the cell numbers were used for normalization of the results.

4.3.2 Cell model limitations

The Caco-2 cell line are derived from an adenocarcinoma and one of the main traits of cancer cells is a metabolic reprogramming, called the Warburg effect. Proliferating cells, such as cancer cells have a higher requirement for reduced carbon and nitrogen and will therefore prioritize creating anabolic precursors rather than maximizing ATP production (Bencze et al., 2020). This means that instead of coupling glycolysis to the TCA cycle, these cells convert pyruvate to lactate (Pavlova & Thompson, 2016). As part of the aim of this study was to examine the respiration and metabolic activity of the cells, this may be of consequence to the results. Due to the Warburg effect, butyrate is also hypothesized to be utilized to a lesser degree in cancer cells (Donohoe et al., 2012). The fatty acid might therefore accumulate in the nucleus, where it acts as an HDAC inhibitor and influences the regulation of gene expression. It is therefore not certain that the fatty acids have the same effects in healthy cells as observed in the cell model. However, the Caco-2 cells express many of the same proteins as normal colonocytes, has been extensively studied and has the benefit of reproducibility (Lea, 2015).

In the human body, the colonocytes are part of a tissue, consisting of different cell types (Allaire et al., 2018). The cells are influenced by substances secreted by nearby cells, such as hormones cytokines and chemokines, as well as by signals from the nervous system (Kagnoff, 2014; Walsh & Zemper, 2019). Being a part of the epithelium, the colonocytes also interact with the components of the gut lumen. Investigating the colonocytes in isolation, will therefore not give a completely realistic impression of how the cells function in the body.

Still, it can provide valuable information as it enables studying the cell type in a way that can easily be controlled.

4.4 Methodological considerations of gene expression quantification

Measuring the levels of RNA can say something about the processes in the cells. Both qPCR and RNA-seq methods entail some challenges when it comes to quantifying gene expression. RNA is in general difficult to work with because it degrades easily, and the different extracts may be of varying quality (Bustin et al., 2005). Ideally, the quality of the samples would be controlled using a bioanalyzer to obtain exact measurements of degradation. Using gel electrophoresis to evaluate the quality is not as exact, but highly degraded samples could be identified and excluded. Due to the poor quality of the RNA isolated from some of the samples, this meant that some treatments had a low number of replicates in the gene expression part of the study.

Both of the gene expression methods are also dependent on cDNA-synthesis, of which the efficiency may vary. The efficiency of the RNA to cDNA conversion is dependent on template abundance (Bustin et al., 2005). The extracts had some variations in RNA concentrations but, all reactions were performed within the range of the kit. The cDNA for qPCR was synthesized using random primers, which attach to multiple sites at each transcript and lead to more than one cDNA per original mRNA, and the majority of cDNA will be from rRNA (Bustin et al., 2005). The cDNA for RNA-seq was also synthesized with random primers, but in this work flow, the samples were first depleted of rRNA.

4.4.1 RNA-seq as a high-throughput method for gene expression screening

RNA-seq is an expensive method and has a comprehensive process of library preparation, which meant that fewer samples were included than with qPCR. The large number of steps in preparation of the libraries, with several rounds of PCR entail a higher risk of introducing variation differences between samples. The samples also had to be handled few at the time, to ensure consistent handling within each batch. Replicates of the same treatments were split between batches to minimize the impact of small variations between batches.

A common issue with RNA-seq is that there are differences in sequencing depth between the samples. Normalization techniques, such as RPKM and TPM have been developed in an

attempt to correct for this, but they are not optimal (Abrams et al., 2019). There is also a problem analyzing reads from very long or very short transcripts, called sample-specific gene length bias which is not corrected for by the traditional normalization methods (Mandelbourn et al., 2019). Another aspect of importance with the method is that different isoforms of genes are included, not all of which lead to functional or even complete transcripts. In qPCR, the primers are designed to match areas of the genes that are important for enzyme function and this method may therefore provide a more relevant estimate of the expression, when they are used to predict functional effects in the cells.

Some deviation is expected between the biological replicates because of the inherent variation between cell samples (Bustin et al., 2005), but the correlations between the TPM values of control samples were very low in this study (appendix C, table C.1). The controls were from different experiment days, which meant that they were at different passages of the cell culture. The BCFA treatments contained fatty acids dissolved in DMSO. The controls that were used in this part of the experiment were also added DMSO, which is toxic at high concentrations, but can also influence cellular processes at lower concentrations (Verheijen et al., 2019). There was however no change in correlation between the two control groups or different passages. The technical replicates showed higher correlations than the biological replicates (appendix C, table C.2), but these also had considerable variations in TPM. This implies that the RNA-seq method introduces variation between samples that does not only reflect the biological difference. The correlation analyses showed that not all of the same genes were detected in all samples, which could signify that the problems are due to low coverage. rRNA depletion was performed to increase the coverage and sensitivity of mRNA, but some rRNA still remained. Degradation of RNA can also impact the gene expression estimates, leading to a shift in relative expression between genes within samples of different quality due to non-uniform degradation (Gallego Romero et al., 2014). Highly degraded samples were excluded from the gene expression part of the experiment, but a lower degree of degradation could not be ruled out by gel electrophoresis.

Even though the RNA-seq results uncovered some technical issues, this is not assumed to significantly influence the credibility of the differential expression analysis. The variation between the controls entail that the gene expression for treated samples would have to be even more dissimilar to be regarded as differentially expressed in the statistical analysis. This could however have resulted in some DE genes not being detected.

4.4.2 qPCR relative quantification by endogenous control

The relative quantification method by qPCR depends on the stable expression of a reference gene to which the expression of GOIs are compared to within each sample. This removes some of the variability that has to do with RNA concentration and cDNA conversion between samples. This normalization method is widely debated as the house-keeping genes that are commonly used as reference genes are not necessarily equally expressed in different samples, depending on the experiment conditions (Kozera & Rapacz, 2013). The accurate quantification with this method also requires primers with maximum amplification efficiency, that are equal for both the GOIs and the reference (Bustin et al., 2005; Livak & Schmittgen, 2001). The efficiencies were close to 100 % for all primers, but *NEIL1* and *NEIL2* showed some deviating R^2 values in the first round (appendix B, table B.1). This may have led to some inaccuracies in the gene expression estimates of these genes in some of the samples.

The gene used as an endogenous control in this study, *GAPDH*, has been shown to have stable expression in Caco-2 cells (Piana et al., 2008). However, the C_q -values of *GAPDH* showed larger variability between samples than some of the GOIs. The variation also seemed unrelated to cell number and input concentration of RNA. There were large variations in relative expression between some of the replicates that corresponded to the most extreme C_q -values of *GAPDH*. The expression of *GAPDH* gene varied between samples in RNA-seq as well but did not correspond with the variation in qPCR. This is probably due to the insensitivity of the RNA-seq method. However, the correlation between expression levels of GOIs in RNA-seq and qPCR was higher with the reference gene normalization than without.

The treatments used in the experiments are hypothesized to influence the metabolism of the cells, and *GAPDH* encodes an enzyme involved in glycolysis. This may be an explanation of the observed variation and suggests that this gene may be inappropriate as a reference gene with this kind of treatment. The qPCR-results with *GAPDH* normalization is used to assess gene expression of GOIs in this thesis as the qPCR method is assumed to be more sensitive than RNA-seq. Further work should include evaluation of different reference genes and the inclusion of more than one reference to get more robust gene expression estimates.

4.5 Physiologic relevance of fatty acid concentrations used in treatment of Caco-2 cells

For practical reasons, concentrations of fatty acids are mostly measured in feces, but as the fatty acids are absorbed by the colonocytes, this makes it complicated to infer the physiologic concentrations in the gut, and to simulate these in vitro. It has been reported that only 5 % of the SCFA produced by bacteria in the gut, reach the feces (Rechkemmer et al., 1988) and measurements in different parts of the gut, done by autopsy of sudden-death victims showed a decrease in SCFA concentrations along the colon (Cummings et al., 1987). This point towards the concentrations being underestimated by fecal measurements. But on the other hand the mucus layer between the IEC and the luminal contents are suggested to lower the concentration experienced by the colonocytes (Donohoe et al., 2012).

In this thesis, the fatty acids were investigated in isolation. The concentrations used were intended to simulate the concentrations of individual fatty acids. This gives an indication of the contribution of each fatty acid, but not how they work when combined, as they are in the human gut.

4.5.1 SCFA treatment concentrations

In this study, the same concentrations were used of all SCFA, although this is not the case in the gut. Acetate concentrations are considerably higher than other SCFA and the propionate concentration is higher than butyrate in the infant gut (Norin et al., 2004). Butyrate concentrations from 11 to 25 mM have been reported in the adult gut (Hamer et al., 2008). In infants, one study reports fecal concentrations increasing from about 0,2 to 13 mM during the first year (Norin et al., 2004). Based on these measurements, the treatment concentration used in this study is closest to the fecal concentrations between 6 and 12 months for butyrate, while lower than concentrations at 1 month for propionate. Because the proportions of fatty acids, especially the important butyrate change a lot during the first year of life, several concentrations should be examined to obtain a better understanding of their influence on the infant gut development. It would be particularly interesting to see if the expression of more genes is significantly influenced with a higher propionate or acetate concentrations.

4.5.2 In vivo BCFA concentrations in the infant gut

Ran-Ressler et al. (2008) have shown that most of the BCFAs in the vernix caseosa, ingested by the fetus, are absorbed and not secreted in meconium. If the main supply of BCFAs is through the diet, the concentrations are expected to decrease along the intestine, as the fatty acids are absorbed by the epithelium. This would lead to a lower concentration of BCFA in the feces compared to the physiologic concentrations in the lumen. As the microbiota develops, it will likely contribute by both consumption and production of BCFAs, but it is difficult to say how this influences the luminal concentration. The treatment concentrations of BCFA used in this study was within the range measured in the feces of 12-month-old children, but the majority of samples contained higher concentrations. Together, these results imply that the observed effects are of relevance to the physiologic conditions in the gut, but also that the physiologic effects may be more prominent. The in vivo concentrations were only measured at an age where most infants have been introduced to solid food, but as BCFAs are ingested before birth and present in human milk, they may be even more prevalent in younger infants. To further elucidate the effects of BCFA in infants, several age groups should be included, and it would also be of relevance to investigate the relationship between BCFA and the microbiota.

5 Value of results and future work

Butyrate was found to influence the mitochondrial activity and had a substantially higher impact on gene expression than the other SCFA at the same concentration. In correspondence with previous research on butyrate, the differentially expressed genes were significantly related to regulation of the cell cycle, which is likely associated with its role as a HDAC inhibitor. In the youngest infants, butyrate is barely present in the gut, while propionate is more prevalent. Propionate showed some similar effects as butyrate on gene expression, although in a smaller magnitude. Propionate also seemed to have effects on mitochondrial activity but did not show the same pattern as butyrate. This could be due to its role as a precursor for gluconeogenesis.

The inclusion of only one SCFA concentration of limits the biological interpretation of the results in this study. Further work should focus on testing the effects of several concentrations and combinations of the fatty acids to provide more context around how the fatty acids are involved in the development of the infant intestinal epithelium.

This study indicates that the BCFA may influence the mitochondrial activity of intestinal epithelial cells, even at low concentrations. Some differentially expressed genes were also identified, which support the claim that the presence of BCFA in the gut can affect the colonocytes. This may be of importance to the infant development as the consumption of BCFA is particularly high right before birth and during breastfeeding. It is however not known how the microbiota influence the BCFA concentrations in the gut. Efforts should be made to elucidate this, as it may influence the interpretation of the effects these fatty acids have on colonocytes.

6 References

- Abrams, Z. B., Johnson, T. S., Huang, K., Payne, P. R. O. & Coombes, K. (2019). A protocol to evaluate RNA sequencing normalization methods. *BMC Bioinformatics*, 20 (Suppl 24): 679. doi: 10.1186/s12859-019-3247-x.
- Abubucker, S., Segata, N., Goll, J., Schubert, A. M., Izard, J., Cantarel, B. L., Rodriguez-Mueller, B., Zucker, J., Thiagarajan, M., Henrissat, B., et al. (2012). Metabolic reconstruction for metagenomic data and its application to the human microbiome. *PLoS Comput Biol*, 8 (6): e1002358. doi: 10.1371/journal.pcbi.1002358.
- Acín-Pérez, R., Fernández-Silva, P., Peleato, M. L., Pérez-Martos, A. & Enriquez, J. A. (2008). Respiratory active mitochondrial supercomplexes. *Mol Cell*, 32 (4): 529-39. doi: 10.1016/j.molcel.2008.10.021.
- Ahmad, M. S., Krishnan, S., Ramakrishna, B. S., Mathan, M., Pulimood, A. B. & Murthy, S. N. (2000). Butyrate and glucose metabolism by colonocytes in experimental colitis in mice. *Gut*, 46 (4): 493-9. doi: 10.1136/gut.46.4.493.
- Albenberg, L., Esipova, T. V., Judge, C. P., Bittinger, K., Chen, J., Laughlin, A., Grunberg, S., Baldassano, R. N., Lewis, J. D., Li, H., et al. (2014). Correlation between intraluminal oxygen gradient and radial partitioning of intestinal microbiota. *Gastroenterology*, 147 (5): 1055-63 e8. doi: 10.1053/j.gastro.2014.07.020.
- Ali, N., Rampazzo, R. C. P., Costa, A. D. T. & Krieger, M. A. (2017). Current Nucleic Acid Extraction Methods and Their Implications to Point-of-Care Diagnostics. *Biomed Res Int*, 2017: 9306564. doi: 10.1155/2017/9306564.
- Allaire, J. M., Crowley, S. M., Law, H. T., Chang, S. Y., Ko, H. J. & Vallance, B. A. (2018). The Intestinal Epithelium: Central Coordinator of Mucosal Immunity. *Trends Immunol*, 39 (9): 677-696. doi: 10.1016/j.it.2018.04.002.
- Archer, S. Y., Meng, S., Shei, A. & Hodin, R. A. (1998). p21(WAF1) is required for butyrate-mediated growth inhibition of human colon cancer cells. *Proc Natl Acad Sci U S A*, 95 (12): 6791-6. doi: 10.1073/pnas.95.12.6791.
- Arya, M., Shergill, I. S., Williamson, M., Gommersall, L., Arya, N. & Patel, H. R. (2005). Basic principles of real-time quantitative PCR. *Expert Rev Mol Diagn*, 5 (2): 209-19. doi: 10.1586/14737159.5.2.209.
- Banerjee, A., Chitnis, U. B., Jadhav, S. L., Bhawalkar, J. S. & Chaudhury, S. (2009). Hypothesis testing, type I and type II errors. *Ind Psychiatry J*, 18 (2): 127-31. doi: 10.4103/0972-6748.62274.
- Banerjee, D., Mandal, S. M., Das, A., Hegde, M. L., Das, S., Bhakat, K. K., Boldogh, I., Sarkar, P. S., Mitra, S. & Hazra, T. K. (2011). Preferential repair of oxidized base damage in the transcribed genes of mammalian cells. *J Biol Chem*, 286 (8): 6006-16. doi: 10.1074/jbc.M110.198796.
- Bencze, G., Bencze, S., Rivera, K. D., Watson, J. D., Orfi, L., Tonks, N. K. & Pappin, D. J. (2020). Mito-oncology agent: fermented extract suppresses the Warburg effect, restores oxidative mitochondrial activity, and inhibits in vivo tumor growth. *Sci Rep*, 10 (1): 14174. doi: 10.1038/s41598-020-71118-3.
- Benjamini, Y. & Hochberg, Y. (1995). Controlling the False Discovery Rate: a Practical and Powerful Approach to Multiple Testing. *J. R. Statist. Soc.*, 57 (1): 289-300.
- Bergman, E. N. (1990). Energy contributions of volatile fatty acids from the gastrointestinal tract in various species. *Physiol Rev*, 70 (2): 567-90. doi: 10.1152/physrev.1990.70.2.567.

- Betarbet, R. & Greenamyre, J. T. (2008). *Parkinson's disease*: Academic Press.
- Bezawork-Geleta, A., Rohlena, J., Dong, L., Pacak, K. & Neuzil, J. (2017). Mitochondrial Complex II: At the Crossroads. *Trends Biochem Sci*, 42 (4): 312-325. doi: 10.1016/j.tibs.2017.01.003.
- Black, D. L. (2003). Mechanisms of Alternative Pre-Messenger RNA Splicing. *Annual Review of Biochemistry*, 72 (1): 291-336. doi: 10.1146/annurev.biochem.72.121801.161720.
- Boffa, L. C., Vidali, G., Mann, R. S. & Allfrey, V. G. (1978). Suppression of histone deacetylation in vivo and in vitro by sodium butyrate. *J Biol Chem*, 253 (10): 3364-6.
- Boulter, N., Suarez, F. G., Schibeci, S., Sunderland, T., Tolhurst, O., Hunter, T., Hodge, G., Handelsman, D., Simanainen, U., Hendriks, E., et al. (2016). A simple, accurate and universal method for quantification of PCR. *BMC Biotechnol*, 16: 27. doi: 10.1186/s12896-016-0256-y.
- Brand, M. D. & Nicholls, D. G. (2011). Assessing mitochondrial dysfunction in cells. *Biochem J*, 435 (2): 297-312. doi: 10.1042/BJ20110162.
- Bridgman, S. L., Azad, M. B., Field, C. J., Haqq, A. M., Becker, A. B., Mandhane, P. J., Subbarao, P., Turvey, S. E., Sears, M. R., Scott, J. A., et al. (2017). Fecal Short-Chain Fatty Acid Variations by Breastfeeding Status in Infants at 4 Months: Differences in Relative versus Absolute Concentrations. *Front Nutr*, 4: 11. doi: 10.3389/fnut.2017.00011.
- Bronner, I. F., Quail, M. A., Turner, D. J. & Swerdlow, H. (2014). Improved Protocols for Illumina Sequencing. *Curr Protoc Hum Genet*, 80: 18.2.1-42. doi: 10.1002/0471142905.hg1802s80.
- Burden, D. W. (2012). Guide to the Disruption of Biological Samples. *Random Primers* (12): 25.
- Bustin, S. A., Benes, V., Nolan, T. & Pfaffl, M. W. (2005). Quantitative real-time RT-PCR--a perspective. *J Mol Endocrinol*, 34 (3): 597-601. doi: 10.1677/jme.1.01755.
- Byndloss, M. X., Olsan, E. E., Rivera-Chavez, F., Tiffany, C. R., Cevallos, S. A., Lokken, K. L., Torres, T. P., Byndloss, A. J., Faber, F., Gao, Y., et al. (2017). Microbiota-activated PPAR-gamma signaling inhibits dysbiotic Enterobacteriaceae expansion. *Science*, 357 (6351): 570-575. doi: 10.1126/science.aam9949.
- Cadena-Herrera, D., Esparza-De Lara, J. E., Ramirez-Ibanez, N. D., Lopez-Morales, C. A., Perez, N. O., Flores-Ortiz, L. F. & Medina-Rivero, E. (2015). Validation of three viable-cell counting methods: Manual, semi-automated, and automated. *Biotechnol Rep (Amst)*, 7: 9-16. doi: 10.1016/j.btre.2015.04.004.
- Carling, D. (2004). The AMP-activated protein kinase cascade--a unifying system for energy control. *Trends Biochem Sci*, 29 (1): 18-24. doi: 10.1016/j.tibs.2003.11.005.
- Chassard, C. & Lacroix, C. (2013). Carbohydrates and the human gut microbiota. *Curr Opin Clin Nutr Metab Care*, 16 (4): 453-60. doi: 10.1097/MCO.0b013e3283619e63.
- Clausen, M. R. & Mortensen, P. B. (1995). Kinetic studies on colonocyte metabolism of short chain fatty acids and glucose in ulcerative colitis. *Gut*, 37 (5): 684-9. doi: 10.1136/gut.37.5.684.
- Cooper, G. M. (2000). Microtubules. In *The Cell: A Molecular Approach*. Sunderland (MA): Sinauer Associates.
- Correa-Oliveira, R., Fachi, J. L., Vieira, A., Sato, F. T. & Vinolo, M. A. (2016). Regulation of immune cell function by short-chain fatty acids. *Clin Transl Immunology*, 5 (4): e73. doi: 10.1038/cti.2016.17.

- Cummings, J. H., Pomare, E. W., Branch, W. J., Naylor, C. P. & Macfarlane, G. T. (1987). Short chain fatty acids in human large intestine, portal, hepatic and venous blood. *Gut*, 28 (10): 1221-7. doi: 10.1136/gut.28.10.1221.
- Da Poian, A. T., El-Bacha, T. & Luz, M. R. M. P. (2010). Nutrient Utilization in Humans: Metabolism Pathways. *Nature Education*, 3 (9).
- Davie, J. R. (2003). Inhibition of histone deacetylase activity by butyrate. *J Nutr*, 133 (7 Suppl): 2485S-2493S. doi: 10.1093/jn/133.7.2485S.
- den Besten, G., Bleeker, A., Gerding, A., van Eunen, K., Havinga, R., van Dijk, T. H., Oosterveer, M. H., Jonker, J. W., Groen, A. K., Reijngoud, D.-J., et al. (2015). Short-Chain Fatty Acids Protect Against High-Fat Diet-Induced Obesity via a PPAR γ -Dependent Switch From Lipogenesis to Fat Oxidation. *Diabetes*. doi: 10.2337/db14-1213
- Dingess, K. A., Valentine, C. J., Ollberding, N. J., Davidson, B. S., Woo, J. G., Summer, S., Peng, Y. M., Guerrero, M. L., Ruiz-Palacios, G. M., Ran-Ressler, R. R., et al. (2017). Branched-chain fatty acid composition of human milk and the impact of maternal diet: the Global Exploration of Human Milk (GEHM) Study. *Am J Clin Nutr*, 105 (1): 177-184. doi: 10.3945/ajcn.116.132464.
- Djafarzadeh, S. & Jakob, S. M. (2017). High-resolution Respirometry to Assess Mitochondrial Function in Permeabilized and Intact Cells. *J Vis Exp* (120). doi: 10.3791/54985.
- Donohoe, D. R., Collins, L. B., Wali, A., Bigler, R., Sun, W. & Bultman, S. J. (2012). The Warburg effect dictates the mechanism of butyrate-mediated histone acetylation and cell proliferation. *Mol Cell*, 48 (4): 612-26. doi: 10.1016/j.molcel.2012.08.033.
- Dunn, J. & Grider, M. H. (2020). *Physiology, Adenosine Triphosphate*. Treasure Island (FL): StatPearls Publishing LLC (accessed: Oct 22).
- Duszka, K., Oresic, M., Le May, C., Konig, J. & Wahli, W. (2017). PPAR γ Modulates Long Chain Fatty Acid Processing in the Intestinal Epithelium. *Int J Mol Sci*, 18 (12). doi: 10.3390/ijms18122559.
- Ehinger, J. K., Piel, S., Ford, R., Karlsson, M., Sjoval, F., Frostner, E. A., Morota, S., Taylor, R. W., Turnbull, D. M., Cornell, C., et al. (2016). Cell-permeable succinate prodrugs bypass mitochondrial complex I deficiency. *Nat Commun*, 7: 12317. doi: 10.1038/ncomms12317.
- Engle, M. J., Goetz, G. S. & Alpers, D. H. (1998). Caco-2 cells express a combination of colonocyte and enterocyte phenotypes. *J Cell Physiol*, 174 (3): 362-9. doi: 10.1002/(SICI)1097-4652(199803)174:3<362::AID-JCP10>3.0.CO;2-B.
- Fabregat, A., Sidiropoulos, K., Viteri, G., Forner, O., Marin-Garcia, P., Arnau, V., D'Eustachio, P., Stein, L. & Hermjakob, H. (2017). Reactome pathway analysis: a high-performance in-memory approach. *BMC Bioinformatics*, 18 (1): 142. doi: 10.1186/s12859-017-1559-2.
- Ferreira, J. A., Ng, K. M. & Sonnenburg, J. L. (2014). The Enteric Two-Step: nutritional strategies of bacterial pathogens within the gut. *Cell Microbiol*, 16 (7): 993-1003. doi: 10.1111/cmi.12300.
- Finotello, F. & Di Camillo, B. (2015). Measuring differential gene expression with RNA-seq: challenges and strategies for data analysis. *Brief Funct Genomics*, 14 (2): 130-42. doi: 10.1093/bfpg/elu035.
- Flint, H. J., Scott, K. P., Duncan, S. H., Louis, P. & Forano, E. (2012a). Microbial degradation of complex carbohydrates in the gut. *Gut Microbes*, 3 (4): 289-306. doi: 10.4161/gmic.19897.

- Flint, H. J., Scott, K. P., Louis, P. & Duncan, S. H. (2012b). The role of the gut microbiota in nutrition and health. *Nat Rev Gastroenterol Hepatol*, 9 (10): 577-89. doi: 10.1038/nrgastro.2012.156.
- Friedman, E. S., Bittinger, K., Esipova, T. V., Hou, L., Chau, L., Jiang, J., Mesaros, C., Lund, P. J., Liang, X., FitzGerald, G. A., et al. (2018). Microbes vs. chemistry in the origin of the anaerobic gut lumen. *Proc Natl Acad Sci U S A*, 115 (16): 4170-4175. doi: 10.1073/pnas.1718635115.
- Fu, W., Liu, Y. & Yin, H. (2019). Mitochondrial Dynamics: Biogenesis, Fission, Fusion, and Mitophagy in the Regulation of Stem Cell Behaviors. *Stem Cells Int*, 2019: 9757201. doi: 10.1155/2019/9757201.
- Fung, K. Y., Cosgrove, L., Lockett, T., Head, R. & Topping, D. L. (2012). A review of the potential mechanisms for the lowering of colorectal oncogenesis by butyrate. *Br J Nutr*, 108 (5): 820-31. doi: 10.1017/S0007114512001948.
- Gallego Romero, I., Pai, A. A., Tung, J. & Gilad, Y. (2014). RNA-seq: impact of RNA degradation on transcript quantification. *BMC Biol*, 12: 42. doi: 10.1186/1741-7007-12-42.
- Garibyan, L. & Avashia, N. (2013). Polymerase chain reaction. *J Invest Dermatol*, 133 (3): 1-4. doi: 10.1038/jid.2013.1.
- Gay, D. A., Sisodia, S. S. & Cleveland, D. W. (1989). Autoregulatory control of beta-tubulin mRNA stability is linked to translation elongation. *Proc Natl Acad Sci U S A*, 86 (15): 5763-7. doi: 10.1073/pnas.86.15.5763.
- Gnaiger, E. (2019). LEAK-respiration: concept-linked terminology of respiratory states. *Mitochondrial Physiology Network*.
- Hamer, H. M., Jonkers, D., Venema, K., Vanhoutvin, S., Troost, F. J. & Brummer, R. J. (2008). Review article: the role of butyrate on colonic function. *Aliment Pharmacol Ther*, 27 (2): 104-19. doi: 10.1111/j.1365-2036.2007.03562.x.
- Hauff, S. & Vetter, W. (2010). Quantification of branched chain fatty acids in polar and neutral lipids of cheese and fish samples. *J Agric Food Chem*, 58 (2): 707-12. doi: 10.1021/jf9034805.
- Hegde, M. L., Hegde, P. M., Bellot, L. J., Mandal, S. M., Hazra, T. K., Li, G. M., Boldogh, I., Tomkinson, A. E. & Mitra, S. (2013). Prereplicative repair of oxidized bases in the human genome is mediated by NEIL1 DNA glycosylase together with replication proteins. *Proc Natl Acad Sci U S A*, 110 (33): E3090-9. doi: 10.1073/pnas.1304231110.
- Hill, B. G., Dranka, B. P., Zou, L., Chatham, J. C. & Darley-Usmar, V. M. (2009). Importance of the bioenergetic reserve capacity in response to cardiomyocyte stress induced by 4-hydroxynonenal. *Biochem J*, 424 (1): 99-107. doi: 10.1042/BJ20090934.
- Hill, B. G., Benavides, G. A., Lancaster, J. R., Jr., Ballinger, S., Dell'Italia, L., Jianhua, Z. & Darley-Usmar, V. M. (2012). Integration of cellular bioenergetics with mitochondrial quality control and autophagy. *Biol Chem*, 393 (12): 1485-1512. doi: 10.1515/hsz-2012-0198.
- Hill, M. J. (1997). Intestinal flora and endogenous vitamin synthesis. *Eur J Cancer Prev*, 6 Suppl 1: S43-5. doi: 10.1097/00008469-199703001-00009.
- Hinnebusch, B. F., Meng, S., Wu, J. T., Archer, S. Y. & Hodin, R. A. (2002). The effects of short-chain fatty acids on human colon cancer cell phenotype are associated with histone hyperacetylation. *J Nutr*, 132 (5): 1012-7. doi: 10.1093/jn/132.5.1012.

- Jang, D. H., Shofer, F. S., Weiss, S. L. & Becker, L. B. (2016). Impairment of mitochondrial respiration following ex vivo cyanide exposure in peripheral blood mononuclear cells. *Clin Toxicol (Phila)*, 54 (4): 303-7. doi: 10.3109/15563650.2016.1139712.
- Jung, T. H., Park, J. H., Jeon, W. M. & Han, K. S. (2015). Butyrate modulates bacterial adherence on LS174T human colorectal cells by stimulating mucin secretion and MAPK signaling pathway. *Nutr Res Pract*, 9 (4): 343-9. doi: 10.4162/nrp.2015.9.4.343.
- Kagnoff, M. F. (2014). The intestinal epithelium is an integral component of a communications network. *J Clin Invest*, 124 (7): 2841-3. doi: 10.1172/JCI75225.
- Kamada, N., Chen, G. Y., Inohara, N. & Nunez, G. (2013). Control of pathogens and pathobionts by the gut microbiota. *Nat Immunol*, 14 (7): 685-90. doi: 10.1038/ni.2608.
- Kaneda, T. (1991). Iso- and anteiso-fatty acids in bacteria: biosynthesis, function, and taxonomic significance. *Microbiol Rev*, 55 (2): 288-302.
- Kelly, C. J., Zheng, L., Campbell, E. L., Saedi, B., Scholz, C. C., Bayless, A. J., Wilson, K. E., Glover, L. E., Kominsky, D. J., Magnuson, A., et al. (2015). Crosstalk between Microbiota-Derived Short-Chain Fatty Acids and Intestinal Epithelial HIF Augments Tissue Barrier Function. *Cell Host Microbe*, 17 (5): 662-71. doi: 10.1016/j.chom.2015.03.005.
- Kim, J., Yang, G., Kim, Y., Kim, J. & Ha, J. (2016). AMPK activators: mechanisms of action and physiological activities. *Exp Mol Med*, 48: e224. doi: 10.1038/emm.2016.16.
- Kozera, B. & Rapacz, M. (2013). Reference genes in real-time PCR. *J Appl Genet*, 54 (4): 391-406. doi: 10.1007/s13353-013-0173-x.
- Kubista, M., Andrade, J. M., Bengtsson, M., Forootan, A., Jonak, J., Lind, K., Sindelka, R., Sjoback, R., Sjogreen, B., Strombom, L., et al. (2006). The real-time polymerase chain reaction. *Mol Aspects Med*, 27 (2-3): 95-125. doi: 10.1016/j.mam.2005.12.007.
- Kurashova, N. A., Madaeva, I. M. & Kolesnikova, L. I. (2019). [Expression of heat shock proteins HSP70 under oxidative stress.]. *Adv Gerontol*, 32 (4): 502-508.
- Lavelle, A. & Sokol, H. (2020). Gut microbiota-derived metabolites as key actors in inflammatory bowel disease. *Nat Rev Gastroenterol Hepatol*, 17 (4): 223-237. doi: 10.1038/s41575-019-0258-z.
- Lea, T. (2015). Caco-2 Cell Line. In Verhoeckx, K., Cotter, P., López-Expósito, I., Kleiveland, C., Lea, T. & Mackie, A. (eds) *The Impact of Food Bioactives on Health*: Springer.
- Lee, O. & O'Brien, P. J. (2010). *Comprehensive Toxicology*. Second Edition ed., vol. 1: Elsevier Science.
- Lefebvre, M., Paulweber, B., Fajas, L., Woods, J., McCrary, C., Colombel, J. F., Najib, J., Fruchart, J. C., Datz, C., Vidal, H., et al. (1999). Peroxisome proliferator-activated receptor gamma is induced during differentiation of colon epithelium cells. *J Endocrinol*, 162 (3): 331-40. doi: 10.1677/joe.0.1620331.
- Levy, E., Mehran, M. & Seidman, E. (1995). Caco-2 cells as a model for intestinal lipoprotein synthesis and secretion. *FASEB J*, 9 (8): 626-35. doi: 10.1096/fasebj.9.8.7768354.
- Li, G. & Reinberg, D. (2011). Chromatin higher-order structures and gene regulation. *Curr Opin Genet Dev*, 21 (2): 175-86. doi: 10.1016/j.gde.2011.01.022.
- Litvak, D. A., Evers, B. M., Hwang, K. O., Hellmich, M. R., Ko, T. C. & Townsend, C. M., Jr. (1998). Butyrate-induced differentiation of Caco-2 cells is associated with apoptosis and early induction of p21Waf1/Cip1 and p27Kip1. *Surgery*, 124 (2): 161-9; discussion 169-70.

- Litvak, Y., Byndloss, M. X., Tsohis, R. M. & Baumler, A. J. (2017). Dysbiotic Proteobacteria expansion: a microbial signature of epithelial dysfunction. *Curr Opin Microbiol*, 39: 1-6. doi: 10.1016/j.mib.2017.07.003.
- Litvak, Y., Byndloss, M. X. & Baumler, A. J. (2018). Colonocyte metabolism shapes the gut microbiota. *Science (New York, N Y)*, 362 (6418).
- Liu, X., Kim, C. N., Yang, J., Jemmerson, R. & Wang, X. (1996). Induction of apoptotic program in cell-free extracts: requirement for dATP and cytochrome c. *Cell*, 86 (1): 147-57. doi: 10.1016/s0092-8674(00)80085-9.
- Livak, K. J. & Schmittgen, T. D. (2001). Analysis of relative gene expression data using real-time quantitative PCR and the 2(-Delta Delta C(T)) Method. *Methods*, 25 (4): 402-8. doi: 10.1006/meth.2001.1262.
- Lozupone, C. A., Stombaugh, J. I., Gordon, J. I., Jansson, J. K. & Knight, R. (2012). Diversity, stability and resilience of the human gut microbiota. *Nature*, 489 (7415): 220-30. doi: 10.1038/nature11550.
- Ma, Y., Temkin, S. M., Hawkrigde, A. M., Guo, C., Wang, W., Wang, X. Y. & Fang, X. (2018). Fatty acid oxidation: An emerging facet of metabolic transformation in cancer. *Cancer Lett*, 435: 92-100. doi: 10.1016/j.canlet.2018.08.006.
- Macfarlane, G. T. & Macfarlane, S. (2007). Models for intestinal fermentation: association between food components, delivery systems, bioavailability and functional interactions in the gut. *Curr Opin Biotechnol*, 18 (2): 156-62. doi: 10.1016/j.copbio.2007.01.011.
- Malago, J. J., Koninkx, J. F., Tooten, P. C., van Liere, E. A. & van Dijk, J. E. (2005). Anti-inflammatory properties of heat shock protein 70 and butyrate on Salmonella-induced interleukin-8 secretion in enterocyte-like Caco-2 cells. *Clin Exp Immunol*, 141 (1): 62-71. doi: 10.1111/j.1365-2249.2005.02810.x.
- Mandelbom, S., Manber, Z., Elroy-Stein, O. & Elkon, R. (2019). Recurrent functional misinterpretation of RNA-seq data caused by sample-specific gene length bias. *PLoS Biol*, 17 (11): e3000481. doi: 10.1371/journal.pbio.3000481.
- Mathews, C. K., Van Holde, K. E., Appling, D. R. & Anthony-Cahill, S. J. (2013). *Biochemistry*. 4th ed.: Pearson.
- Mendelson, Y. (2012). Biomedical Sensors. In *Introduction to Biomedical Engineering*, pp. 640-645: Academic Press.
- Miao, W., Wu, X., Wang, K., Wang, W., Wang, Y., Li, Z., Liu, J., Li, L. & Peng, L. (2016). Sodium Butyrate Promotes Reassembly of Tight Junctions in Caco-2 Monolayers Involving Inhibition of MLCK/MLC2 Pathway and Phosphorylation of PKCbeta2. *Int J Mol Sci*, 17 (10). doi: 10.3390/ijms17101696.
- Milani, C., Duranti, S., Bottacini, F., Casey, E., Turrone, F., Mahony, J., Belzer, C., Delgado Palacio, S., Arboleya Montes, S., Mancabelli, L., et al. (2017). The First Microbial Colonizers of the Human Gut: Composition, Activities, and Health Implications of the Infant Gut Microbiota. *Microbiol Mol Biol Rev*, 81 (4). doi: 10.1128/MMBR.00036-17.
- Nicholls, D. G. & Ferguson, S. J. (2002). *Bioenergetics 3*. 3rd ed. ed. Bioenergetics three. San Diego, Calif.: Academic Press.
- Noah, T. K., Donahue, B. & Shroyer, N. F. (2011). Intestinal development and differentiation. *Exp Cell Res*, 317 (19): 2702-10. doi: 10.1016/j.yexcr.2011.09.006.
- Norin, E., Midtvedt, T. & Björkstén, B. (2004). Development of Faecal Short-Chain Fatty Acid Pattern during the First Year of Life in Estonian and Swedish Infants. *Microbial Ecology in Health and Disease*, 16:1: 8-12. doi: 10.1080/08910600410026364.

- Orchel, A., Dzierzewicz, Z., Parfiniewicz, B., Weglarz, L. & Wilczok, T. (2005). Butyrate-induced differentiation of colon cancer cells is PKC and JNK dependent. *Dig Dis Sci*, 50 (3): 490-8. doi: 10.1007/s10620-005-2463-6.
- Park, S. Y., Kim, D. & Kee, S. H. (2019). Metformin-activated AMPK regulates beta-catenin to reduce cell proliferation in colon carcinoma RKO cells. *Oncol Lett*, 17 (3): 2695-2702. doi: 10.3892/ol.2019.9892.
- Parker, A. L., Kavallaris, M. & McCarroll, J. A. (2014). Microtubules and their role in cellular stress in cancer. *Front Oncol*, 4: 153. doi: 10.3389/fonc.2014.00153.
- Patel, V. A., Massenburg, D., Vujicic, S., Feng, L., Tang, M., Litbarg, N., Antoni, A., Rauch, J., Lieberthal, W. & Levine, J. S. (2015). Apoptotic cells activate AMP-activated protein kinase (AMPK) and inhibit epithelial cell growth without change in intracellular energy stores. *J Biol Chem*, 290 (37): 22352-69. doi: 10.1074/jbc.M115.667345.
- Pavlova, N. N. & Thompson, C. B. (2016). The Emerging Hallmarks of Cancer Metabolism. *Cell Metab*, 23 (1): 27-47. doi: 10.1016/j.cmet.2015.12.006.
- Peng, L., Li, Z. R., Green, R. S., Holzman, I. R. & Lin, J. (2009). Butyrate enhances the intestinal barrier by facilitating tight junction assembly via activation of AMP-activated protein kinase in Caco-2 cell monolayers. *J Nutr*, 139 (9): 1619-25. doi: 10.3945/jn.109.104638.
- Penn, R., Ward, B. J., Strande, L. & Maurer, M. (2018). Review of synthetic human faeces and faecal sludge for sanitation and wastewater research. *Water Res*, 132: 222-240. doi: 10.1016/j.watres.2017.12.063.
- Peterson, L. W. & Artis, D. (2014). Intestinal epithelial cells: regulators of barrier function and immune homeostasis. *Nat Rev Immunol*, 14 (3): 141-53. doi: 10.1038/nri3608.
- Piana, C., Wirth, M., Gerbes, S., Viernstein, H., Gabor, F. & Toegel, S. (2008). Validation of reference genes for qPCR studies on Caco-2 cell differentiation. *Eur J Pharm Biopharm*, 69 (3): 1187-92. doi: 10.1016/j.ejpb.2008.03.008.
- Pignata, S., Maggini, L., Zarrilli, R., Rea, A. & Acquaviva, A. M. (1994). The enterocyte-like differentiation of the Caco-2 tumor cell line strongly correlates with responsiveness to cAMP and activation of kinase A pathway. *Cell Growth Differ*, 5 (9): 967-73.
- Pinto, D., Gregorieff, A., Begthel, H. & Clevers, H. (2003). Canonical Wnt signals are essential for homeostasis of the intestinal epithelium. *Genes Dev*, 17 (14): 1709-13. doi: 10.1101/gad.267103.
- QIAGEN. (2020). *CLC Genomics Workbench User Manual*. Aarhus, Denmark.
- Ran-Ressler, R. R., Devapatla, S., Lawrence, P. & Brenna, J. T. (2008). Branched chain fatty acids are constituents of the normal healthy newborn gastrointestinal tract. *Pediatr Res*, 64 (6): 605-9. doi: 10.1203/PDR.0b013e318184d2e6.
- Ran-Ressler, R. R., Khailova, L., Arganbright, K. M., Adkins-Rieck, C. K., Jouni, Z. E., Koren, O., Ley, R. E., Brenna, J. T. & Dvorak, B. (2011). Branched chain fatty acids reduce the incidence of necrotizing enterocolitis and alter gastrointestinal microbial ecology in a neonatal rat model. *PLoS One*, 6 (12): e29032. doi: 10.1371/journal.pone.0029032.
- Ran-Ressler, R. R., Glahn, R. P., Bae, S. & Brenna, J. T. (2013). Branched-chain fatty acids in the neonatal gut and estimated dietary intake in infancy and adulthood. *Nestle Nutr Inst Workshop Ser*, 77: 133-43. doi: 10.1159/000351396.
- Ran-Ressler, R. R., Bae, S., Lawrence, P., Wang, D. H. & Brenna, J. T. (2014). Branched-chain fatty acid content of foods and estimated intake in the USA. *Br J Nutr*, 112 (4): 565-72. doi: 10.1017/S0007114514001081.

- Raudvere, U., Kolberg, L., Kuzmin, I., Arak, T., Adler, P., Peterson, H. & Vilo, J. (2019). g:Profiler: a web server for functional enrichment analysis and conversions of gene lists (2019 update). *Nucleic Acids Res*, 47 (W1): W191-W198. doi: 10.1093/nar/gkz369.
- Rechkemmer, G., Rönnau, K. & Engelhardt, W. (1988). Fermentation of polysaccharides and absorption of short chain fatty acids in the mammalian hindgut. *Comparative Biochemistry and Physiology Part A: Physiology*, 90 (4): 563-568.
- Rennoll, S. & Yochum, G. (2015). Regulation of MYC gene expression by aberrant Wnt/beta-catenin signaling in colorectal cancer. *World J Biol Chem*, 6 (4): 290-300. doi: 10.4331/wjbc.v6.i4.290.
- Rios-Covian, D., Ruas-Madiedo, P., Margolles, A., Gueimonde, M., de Los Reyes-Gavilan, C. G. & Salazar, N. (2016). Intestinal Short Chain Fatty Acids and their Link with Diet and Human Health. *Front Microbiol*, 7: 185. doi: 10.3389/fmicb.2016.00185.
- Robinson, M. D. & Oshlack, A. (2010). A scaling normalization method for differential expression analysis of RNA-seq data. *Genome Biol*, 11 (3): R25. doi: 10.1186/gb-2010-11-3-r25.
- Roediger, W. E. (1980). Role of anaerobic bacteria in the metabolic welfare of the colonic mucosa in man. *Gut*, 21 (9): 793-8. doi: 10.1136/gut.21.9.793.
- Roediger, W. E. (1982). Utilization of nutrients by isolated epithelial cells of the rat colon. *Gastroenterology*, 83 (2): 424-9.
- Rusyn, I., Asakura, S., Pachkowski, B., Bradford, B. U., Denissenko, M. F., Peters, J. M., Holland, S. M., Reddy, J. K., Cunningham, M. L. & Swenberg, J. A. (2004). Expression of base excision DNA repair genes is a sensitive biomarker for in vivo detection of chemical-induced chronic oxidative stress: identification of the molecular source of radicals responsible for DNA damage by peroxisome proliferators. *Cancer Res*, 64 (3): 1050-7. doi: 10.1158/0008-5472.can-03-3027.
- Sanchez-Alcazar, J. A., Khodjakov, A. & Schneider, E. (2001). Anticancer drugs induce increased mitochondrial cytochrome c expression that precedes cell death. *Cancer Res*, 61 (3): 1038-44.
- Scialo, F., Fernandez-Ayala, D. J. & Sanz, A. (2017). Role of Mitochondrial Reverse Electron Transport in ROS Signaling: Potential Roles in Health and Disease. *Front Physiol*, 8: 428. doi: 10.3389/fphys.2017.00428.
- Siliakus, M. F., van der Oost, J. & Kengen, S. W. M. (2017). Adaptations of archaeal and bacterial membranes to variations in temperature, pH and pressure. *Extremophiles*, 21 (4): 651-670. doi: 10.1007/s00792-017-0939-x.
- Sims, D., Sudbery, I., Illott, N. E., Heger, A. & Ponting, C. P. (2014). Sequencing depth and coverage: key considerations in genomic analyses. *Nat Rev Genet*, 15 (2): 121-32. doi: 10.1038/nrg3642.
- Smith, P. M., Howitt, M. R., Panikov, N., Michaud, M., Gallini, C. A., Bohlooly, Y. M., Glickman, J. N. & Garrett, W. S. (2013). The microbial metabolites, short-chain fatty acids, regulate colonic Treg cell homeostasis. *Science*, 341 (6145): 569-73. doi: 10.1126/science.1241165.
- Sun, M., Wu, W., Liu, Z. & Cong, Y. (2017). Microbiota metabolite short chain fatty acids, GPCR, and inflammatory bowel diseases. *J Gastroenterol*, 52 (1): 1-8. doi: 10.1007/s00535-016-1242-9.
- Tan, S. C. & Yiap, B. C. (2009). DNA, RNA, and protein extraction: the past and the present. *J Biomed Biotechnol*, 2009: 574398. doi: 10.1155/2009/574398.

- Taormina, V. M., Unger, A. L., Schiksnis, M. R., Torres-Gonzalez, M. & Kraft, J. (2020). Branched-Chain Fatty Acids-An Underexplored Class of Dairy-Derived Fatty Acids. *Nutrients*, 12 (9). doi: 10.3390/nu12092875.
- Thursby, E. & Juge, N. (2017). Introduction to the human gut microbiota. *Biochem J*, 474 (11): 1823-1836. doi: 10.1042/BCJ20160510.
- Topping, D. L. & Clifton, P. M. (2001). Short-chain fatty acids and human colonic function: roles of resistant starch and nonstarch polysaccharides. *Physiol Rev*, 81 (3): 1031-64. doi: 10.1152/physrev.2001.81.3.1031.
- Tretter, L., Patocs, A. & Chinopoulos, C. (2016). Succinate, an intermediate in metabolism, signal transduction, ROS, hypoxia, and tumorigenesis. *Biochim Biophys Acta*, 1857 (8): 1086-1101. doi: 10.1016/j.bbabi.2016.03.012.
- Turnbaugh, P. J., Hamady, M., Yatsunencko, T., Cantarel, B. L., Duncan, A., Ley, R. E., Sogin, M. L., Jones, W. J., Roe, B. A., Affourtit, J. P., et al. (2009). A core gut microbiome in obese and lean twins. *Nature*, 457 (7228): 480-4. doi: 10.1038/nature07540.
- Turrens, J. F. (1997). Superoxide production by the mitochondrial respiratory chain. *Biosci Rep*, 17 (1): 3-8. doi: 10.1023/a:1027374931887.
- van der Knaap, J. A. & Verrijzer, C. P. (2016). Undercover: gene control by metabolites and metabolic enzymes. *Genes Dev*, 30 (21): 2345-2369. doi: 10.1101/gad.289140.116.
- Van Houten, B., Santa-Gonzalez, G. A. & Camargo, M. (2018). DNA repair after oxidative stress: current challenges. *Curr Opin Toxicol*, 7: 9-16. doi: 10.1016/j.cotox.2017.10.009.
- Verheijen, M., Lienhard, M., Schrooders, Y., Clayton, O., Nudischer, R., Boerno, S., Timmermann, B., Selevsek, N., Schlapbach, R., Gmuender, H., et al. (2019). DMSO induces drastic changes in human cellular processes and epigenetic landscape in vitro. *Sci Rep*, 9 (1): 4641. doi: 10.1038/s41598-019-40660-0.
- Wagner, G. P., Kin, K. & Lynch, V. J. (2012). Measurement of mRNA abundance using RNA-seq data: RPKM measure is inconsistent among samples. *Theory Biosci*, 131 (4): 281-5. doi: 10.1007/s12064-012-0162-3.
- Walsh, K. T. & Zemper, A. E. (2019). The Enteric Nervous System for Epithelial Researchers: Basic Anatomy, Techniques, and Interactions With the Epithelium. *Cell Mol Gastroenterol Hepatol*, 8 (3): 369-378. doi: 10.1016/j.jcmgh.2019.05.003.
- Wenz, T. (2013). Regulation of mitochondrial biogenesis and PGC-1alpha under cellular stress. *Mitochondrion*, 13 (2): 134-42. doi: 10.1016/j.mito.2013.01.006.
- Westermann, A. J., Gorski, S. A. & Vogel, J. (2012). Dual RNA-seq of pathogen and host. *Nat Rev Microbiol*, 10 (9): 618-30. doi: 10.1038/nrmicro2852.
- Wold, S. (1987). Principal Component Analysis. *Chemometrics and Intelligent Laboratory Systems*, 2: 37-52.
- Yamamoto, H., Morino, K., Mengistu, L., Ishibashi, T., Kiriya, K., Ikami, T. & Maegawa, H. (2016). Amla Enhances Mitochondrial Spare Respiratory Capacity by Increasing Mitochondrial Biogenesis and Antioxidant Systems in a Murine Skeletal Muscle Cell Line. *Oxid Med Cell Longev*, 2016: 1735841. doi: 10.1155/2016/1735841.
- Yan, Y., Wang, Z., Greenwald, J., Kothapalli, K. S., Park, H. G., Liu, R., Mendralla, E., Lawrence, P., Wang, X. & Brenna, J. T. (2017). BCFA suppresses LPS induced IL-8 mRNA expression in human intestinal epithelial cells. *Prostaglandins Leukot Essent Fatty Acids*, 116: 27-31. doi: 10.1016/j.plefa.2016.12.001.

- Zhang, J., Wang, X., Vikash, V., Ye, Q., Wu, D., Liu, Y. & Dong, W. (2016). ROS and ROS-Mediated Cellular Signaling. *Oxid Med Cell Longev*, 2016: 4350965. doi: 10.1155/2016/4350965.
- Zhang, Y., Li, N., Caron, C., Matthias, G., Hess, D., Khochbin, S. & Matthias, P. (2003). HDAC-6 interacts with and deacetylates tubulin and microtubules in vivo. *EMBO J*, 22 (5): 1168-79. doi: 10.1093/emboj/cdg115.
- Zhao, S., Zhang, Y., Gamini, R., Zhang, B. & von Schack, D. (2018). Evaluation of two main RNA-seq approaches for gene quantification in clinical RNA sequencing: polyA+ selection versus rRNA depletion. *Sci Rep*, 8 (1): 4781. doi: 10.1038/s41598-018-23226-4.
- Zhao, W., He, X., Hoadley, K. A., Parker, J. S., Hayes, D. N. & Perou, C. M. (2014). Comparison of RNA-Seq by poly (A) capture, ribosomal RNA depletion, and DNA microarray for expression profiling. *BMC Genomics*, 15: 419. doi: 10.1186/1471-2164-15-419.
- Zhao, Y., Wang, Z. B. & Xu, J. X. (2003). Effect of cytochrome c on the generation and elimination of O₂*- and H₂O₂ in mitochondria. *J Biol Chem*, 278 (4): 2356-60. doi: 10.1074/jbc.M209681200.
- Zweibaum, A. (1991). Differentiation of Human Colon Cancer-Cells. *Pharmaceutical Applications of Cell and Tissue Culture to Drug Transport*, 218: 27-37.

Appendix A: RNA qualification

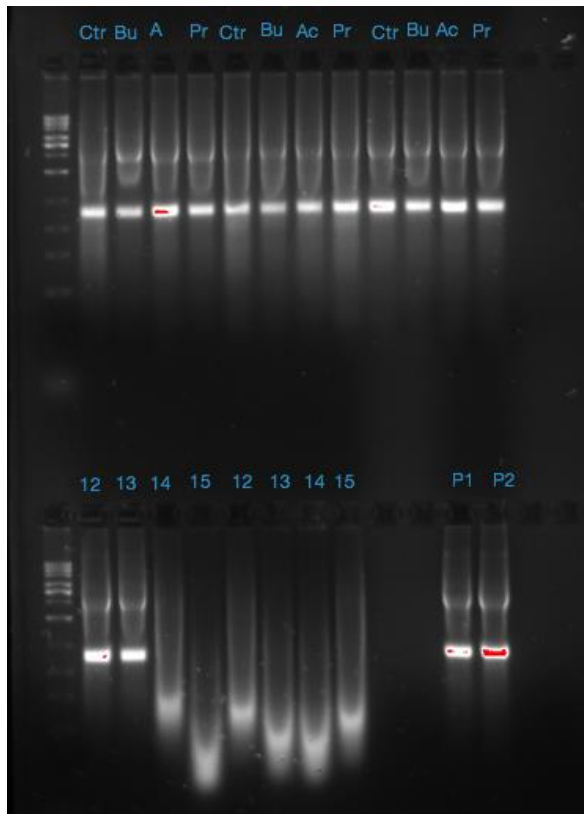


Figure A.1 Gel electrophoresis of first round RNA samples, together with two pilot samples (P1 and P2). The first well contains a 1kb ladder.

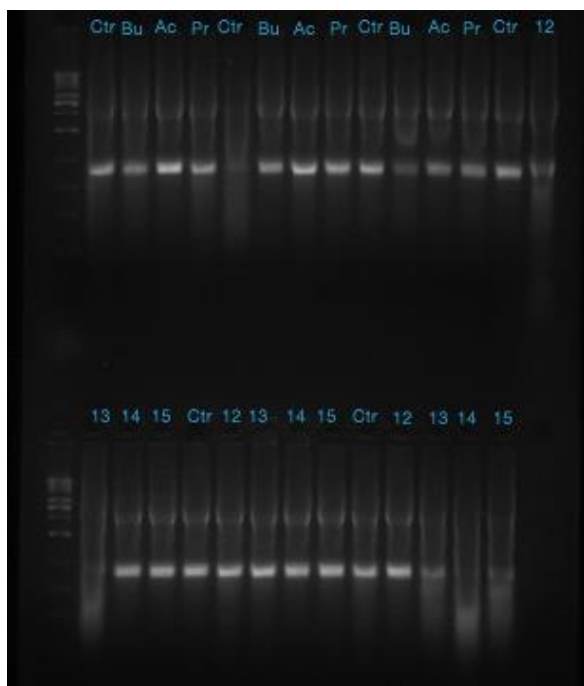


Figure A.2 Gel electrophoresis of the second round of RNA samples. The first well contains a 1kb ladder.

Appendix B: Primer Efficiencies

Table B.1 Efficiencies and R^2 values for primer pairs in each of the two rounds of qPCR

	ROUND 1		ROUND 2	
	EFFICIENCY	R^2	EFFICIENCY	R^2
GAPDH	0,97	0,99	1,09	0,99
SDHB	0,99	0,99	1,10	0,99
NDUFA9	1,00	0,99	0,96	0,99
MT-ND2	1,04	0,99	1,00	0,99
MT-ND6	1,03	0,99	1,01	0,99
CYCS	1,00	0,99	1,10	0,99
NEIL1	0,95	0,98	0,94	0,99
NEIL2	1,12	0,95	1,02	0,99
OGG1	0,93	0,99	1,10	0,99

Appendix C: Correlations between controls in RNA-seq

Table C.1 R^2 values for pairwise correlations of TPM values between control samples. The samples used as controls against SCFA-treatment are named with S, while the controls compared with BCFA-treatment are named with B. The numbers indicate different biological replicates. The passage number is indicated in the parenthesis.

	CTR-S1 (P8)	CTR-S3 (P10)	CTR-B1 (P12)	CTR-B2 (P13)	CTR-B3 (P14)
CTR-S1 (P8)					
CTR-S3 (P10)	0,59				
CTR-B1 (P12)	0,48	0,48			
CTR-B2 (P13)	0,60	0,58	0,46		
CTR-B3 (P14)	0,59	0,58	0,48	0,58	

Table C.2 R^2 values for correlations between technical replicates of an un-treated sample (CTR-S1) and a butyrate-treated sample (BU-1).

	R^2
CTR-S1	0,71
BU-1	0,76

Appendix D: Differentially expressed transcripts/genes

Table D.1 Differentially expressed transcripts in cells treated with 4 mM SCFA or 40 μ M BCFA for 24 hours compared to the complete set of control samples (N=5). Transcripts that could not be associated with a gene by g:Convert are marked with "None". The number of biological replicates (N) for each treatment is showed in parenthesis in the first column.

TREATMENT	TRANSCRIPTS UP- REGULATED	GENE NAME	TRANSCRIPTS DOWN- REGULATED	GENE NAME
ACETATE (N=3)	NM_001127193.2	CNBP	XM_011538771.2	KMT2D
	NM_006534.4	NCOA3	NM_001096.3	ACLY
PROPIONATE (N=3)	NM_013390.3	CEMIP2	NM_006738.6	AKAP13
	NM_031313.3	ALPG	NM_001136204.3	RCC2
	NM_006009.4	TUBA1A	NM_001291862.3	IGF2
	NM_003897.4	IER3	NM_001382506.1	None
	NM_004419.4	DUSP5	NM_002140.4	HNRNPK
	NM_003088.4	FSCN1	XM_006712636.3	UGGT1
	NM_006516.4	SLC2A1	XR_936532.2	LAMA5
	NM_012244.4	SLC7A8		
	NM_005562.3	LAMC2		
	NM_005542.6	INSIG1		
	NM_003979.4	GPRC5A		
	NM_001730.5	KLF5		
BUTYRATE (N=3)	NM_004055.5	CAPN5	NM_001291862.3	IGF2
	NM_002507.4	NGFR	NM_001193508.1	REST
	XM_017020539.1	SACS	NM_001171136.2	ZBED1
	NM_138420.4	AHNAK2	NM_001330655.2	DDAH1
	NM_001042544.1	LTBP4	NM_001330292.2	MTA2
	NM_020645.3	NRIP3	XR_923001.3	BUB1
	NM_005909.5	MAP1B	XM_017004714.1	ANAPC1
	NM_001145056.2	SLC44A2	NR_073007.2	CDK2AP1
	NM_001172896.2	CAV1	NM_001330439.1	SMARCD2
	NM_173542.4	PLBD2	NM_001040458.3	ERAP1
	NM_001199097.2	BAIAP3	NM_005170.2	ASCL2
	NM_001008738.3	FNIP1	NM_001101677.2	SOHLH1
	NM_152296.5	ATP1A3	XM_017001046.1	CACYBP
	NM_001307936.2	SLC38A2	NR_024345.1	HNF1A-AS1
	NM_181742.3	ORC4	NM_012206.3	HAVCR1
	NM_001206938.2	TCAF1	XM_005245305.5	KIRREL1
	NM_018084.5	CCDC88A	NM_016391.8	NOP16
	NM_007365.3	PADI2	NM_000458.4	HNF1B
	NM_203468.3	ENTPD2	NM_001040022.1	SIRPA
	XM_017000085.2	TXNIP	NM_014788.4	TRIM14
	NM_153713.3	LIX1L	NM_003580.4	NSMAF
	NM_198580.3	SLC27A1	XR_936532.2	LAMA5
	NM_005794.4	DHRS2	NR_146718.1	LINC02038
	NM_001166286.2	RGMA	NM_001042539.3	MAZ
	NM_002305.4	LGALS1	NM_033260.4	FOXQ1
	NM_001678.5	ATP1B2	XM_024446022.1	HAVCR1
	NM_031313.3	ALPG	NM_003223.3	TFAP4

NM_006087.4	TUBB4A	NM_002181.4	IHH
NM_006009.4	TUBA1A	NM_001145155.2	NR2F2
NM_020820.4	PREX1	NM_002083.4	GPX2
NM_007074.4	CORO1A	NM_001164758.1	PRKAR1B
NM_020134.4	DPYSL5	NM_001244638.2	ARID5B
NM_206901.3	RTN2	XM_005269037.4	NUP107
NM_004522.3	KIF5C	XM_017004005.1	ITGA6
NM_002736.3	PRKAR2B	NM_199141.2	CARM1
NM_001005404.4	YPEL2	NM_145177.3	DHRXSX
NM_020309.4	SLC17A7	NM_002028.4	FNTB
NM_001303263.1	ATP1B2	XM_011529183.3	None
XM_017009342.1	CYFIP2	NM_005504.7	BCAT1
NM_031476.4	CRISPLD2	XM_017011137.1	ZBTB2
NM_001256213.1	ATP1A3	NM_012154.5	AGO2
NM_000399.5	EGR2	NM_021021.4	SNTB1
XR_001751594.1	None	NM_002546.4	TNFRSF11B
NM_173798.4	ZCCHC12	NM_004500.4	None
XR_939545.3	None	NM_001071.4	TYMS
NM_004750.5	CRLF1	NM_138408.4	GTF3C6
NM_001377486.1	GAN	NR_046110.1	LINC01123
XM_005271355.3	KDM4A	NM_001199984.1	NDUFS1
NM_006688.5	C1QL1	NM_032822.3	FAM136A
XR_001750027.1	None	NM_021158.4	TRIB3
NM_003811.4	TNFSF9	NM_001080392.2	DENND11
NM_006500.3	MCAM	NM_017671.5	FERMT1
XR_001750029.1	None	NM_175914.4	HNF4A
NM_006389.5	HYOU1	NM_006546.4	IGF2BP1
NM_001140.5	ALOX15	NM_030812.3	ACTL8
NM_182705.2	RFLNB	NM_001235.5	SERPINH1
NM_000389.5	CDKN1A	NM_033000.4	GTF2I
NR_135691.1	LINC02204	XM_011524201.2	IGF2BP1
NM_178500.4	PHOSPHO1	NM_024098.4	CCDC86
NM_000093.5	COL5A1	NM_014503.3	UTP20
NM_001172437.2	PEG10	NM_138370.3	PKDCC
NM_002516.4	NOVA2	NM_001330247.1	HNRNPA3
NM_006336.4	ZER1	NM_001007026.2	ATN1
NM_001004128.2	QSOX1	NM_005139.3	ANXA3
NM_019106.5	SEPTIN3	NM_080833.3	RBBP8NL
NM_001313972.2	TXNIP	NM_004496.5	FOXA1
NM_002135.4	NR4A1	NM_003483.6	None
NM_198475.3	FAM171A2	NM_024534.5	ERVMER34-
NM_001166288.2	RGMA	NM_001039111.3	1
NM_006176.3	NRGN	NM_002653.5	TRIM71
XM_006715960.3	TSPAN33	XM_005249581.5	PITX1
NM_001371242.2	CRYBG1	NM_003786.4	AGR2
NM_138961.3	ESAM	NM_005558.4	ABCC3
NR_002819.4	MALAT1	NM_174908.4	LAD1
NM_004973.4	JARID2	NM_002940.3	CCDC50
NM_013390.3	CEMIP2	NM_003132.3	ABCE1
XM_017019247.1	NR4A1	NM_014766.5	SRM

NM_005953.5	MT2A	NM_007208.4	SCRN1
NM_006262.4	PRPH	NM_002467.6	MRPL3
NM_173582.6	PGM2L1	NM_153705.5	MYC
NM_004362.3	CLGN	NM_000384.3	POGLUT3
NM_002970.3	SAT1	NM_014825.3	APOB
NM_000088.4	COL1A1	NM_004494.3	URB1
NM_001160125.1	KLF6	NM_003592.3	HDGF
NM_001079871.1	HAP1	XM_017006798.2	CUL1
NM_006472.6	TXNIP	NM_006401.3	CHDH
NM_173157.3	NR4A1	NM_002901.4	ANP32B
NM_001024401.3	SBK1	XM_005251853.3	RCN1
NM_001126049.2	None	NM_001330212.1	ECPAS
NM_183376.3	ARRDC4	NM_001759.4	PSMC1
XR_001750107.1	DHRS2	NM_001144994.2	CCND2
NM_001876.4	CPT1A	NM_080388.3	C2orf72
NR_119376.1	FER1L4	NM_024662.3	S100A16
NM_001874.4	CPM	NM_020300.5	NAT10
NM_001291738.1	CD24	NM_182762.4	MGST1
NM_002373.6	MAP1A	NM_017755.6	MACC1
NM_021979.3	HSPA2	NR_027700.3	NSUN2
NM_006086.4	TUBB3	NM_000392.5	NOP56
NR_027001.1	GOLGA2P7	NM_000305.3	ABCC2
XR_002958258.1	None	NM_003290.3	PON2
NM_001039141.3	TRIOBP	NM_003315.4	TPM4
NM_001632.5	ALPP	NM_006408.4	DNAJC7
NM_004430.3	EGR3	NM_003714.2	AGR2
NM_006270.5	RRAS	NM_006936.3	STC2
NR_015379.3	UCA1	NM_014874.4	SUMO3
NM_003088.4	FSCN1	NM_033119.5	MFN2
NM_006079.5	CITED2	NM_015131.3	NKD1
NM_001080497.3	MEGF9	NM_005782.4	WDR43
NR_002774.3	HTR7P1	NM_002586.5	ALYREF
NM_014398.4	LAMP3	NM_005891.3	PBX2
XR_001737203.1	ATF3	NM_005573.4	ACAT2
NR_160936.1	None	NM_024658.4	LMNB1
NM_005456.4	MAPK8IP1	NM_001284389.2	IPO4
XM_024452421.1	SAT1	NM_006015.6	NOLC1
NM_001958.5	EEF1A2	NM_001363661.1	ARID1A
NM_004417.4	DUSP1	NM_018128.5	HMGB1
NM_001901.4	None	NM_004044.7	TSR1
NR_144568.1	MALAT1	NM_015339.5	ATIC
NM_001831.4	CLU	XM_024452040.1	ADNP
NM_004040.4	RHOB	NM_006885.4	None
NM_004419.4	DUSP5	NR_146154.1	ZFH3
NM_002228.4	JUN	NM_053056.3	None
NM_006317.5	BASP1	NM_006645.2	CCND1
NM_001039844.3	ACBD7	NM_006108.4	STARD10
NR_131012.1	NEAT1	NM_001102371.2	SPON1
NM_032409.3	PINK1	NM_022731.5	FOXRED2
NM_000434.4	NEU1	NM_001037738.3	NUCKS1

NM_001124.3	ADM	NM_004728.4	NPM1
NM_002070.4	GNAI2	NM_000492.4	DDX21
NM_006026.4	H1-10	NM_031266.3	CFTR
NM_001042465.3	PSAP	XM_017029908.1	HNRNPAB
NR_028272.1	NEAT1	NM_198976.4	OGT
NM_033049.4	MUC13	NM_002157.3	NELFCD
NM_001304717.5	PTEN	NM_015659.3	HSPE1
NM_005252.4	FOS	NM_001032283.3	RSL1D1
NR_027889.1	TMEM189	NM_006325.5	TMPO
NM_004433.5	ELF3	NM_007192.4	RAN
NM_021960.5	MCL1	NM_014573.3	SUPT16H
NM_004907.3	IER2	NM_012073.5	TMEM97
NM_006931.3	SLC2A3	NM_004134.7	CCT5
NM_003107.3	SOX4	NM_002265.6	HSPA9
NM_032421.3	CLIP2		KPNB1
NM_001040152.2	PEG10		
NM_003897.4	IER3		
XM_017018028.1	PNPLA2		
NM_001184962.2	PEG10		
NM_002276.5	KRT19		
NM_003468.4	FZD5		
NM_178012.5	TUBB2B		
NM_005242.6	F2RL1		
XM_017013892.1	EPPK1		
NM_001286968.2	JUND		
NM_020928.2	ZSWIM6		
NM_014423.4	AFF4		
NM_002087.4	GRN		
NM_005354.6	JUND		
NM_001172438.3	PEG10		
NM_012232.6	CAVIN1		
NM_203372.3	ACSL3		
NM_001684.5	ATP2B4		
NM_003255.5	TIMP2		
NM_004457.5	ACSL3		
NR_037688.3	ACTG1		
NM_001456.3	FLNA		
NM_015161.3	ARL6IP1		
NM_005516.6	HLA-E		
NM_130787.3	AP2A1		
NM_001300.6	KLF6		
NM_016185.4	JPT1		
NM_000235.4	LIPA		
NM_003258.5	TK1		
NM_001430.5	EPAS1		
NM_001614.5	ACTG1		
NM_020412.5	CHMP1B		
NM_000127.3	EXT1		
NM_004691.5	ATP6V0D1		
NM_001360016.2	G6PD		

	NM_005542.6	INSIG1		
	NM_000405.5	GM2A		
	NM_003979.4	GPRC5A		
	NM_012244.4	SLC7A8		
	NM_005320.3	H1-3		
	NM_005345.6	HSPA1A		
	NM_022818.5	MAP1LC3B		
	NM_080725.3	SRXN1		
	NM_005318.4	H1-0		
	NM_181697.3	PRDX1		
	NM_001554.5	CCN1		
	NM_006617.2	NES		
	NM_014000.3	VCL		
	NM_006471.4	MYL12A		
	NM_001145064.3	CASTOR2		
	NM_001457.4	FLNB		
	NM_004736.4	XPR1		
	NM_002778.4	PSAP		
	NM_080677.3	DYNLL2		
	NM_001730.5	KLF5		
	NM_021814.5	ELOVL5		
	NM_001657.4	AREG		
	NM_002076.4	GNS		
	NM_004096.5	EIF4EBP2		
	NM_006835.3	CCNI		
12-MTD (N=2)			NM_001010972.2	ZYX
13-MTD (N=1)			NM_001379.4	DNMT1
			NM_005245.4	FAT1
14-MHD (N=2)			NM_004302.5	ACVR1B

Appendix E: Top pathways with propionate-treatment

Table E.1 Top 20 pathways overrepresented by differentially genes in Caco-2 cells after treatment with 4 mM propionate for 24 hours.

PATHWAY NAME	ENTITIES FDR
Insulin-like Growth Factor-2 mRNA Binding Proteins (IGF2BPs/IMPs/VICKZs) bind RNA	7,37E-02
Interleukin-4 and Interleukin-13 signaling	7,87E-02
Laminin interactions	1,08E-01
MET activates PTK2 signaling	1,08E-01
MET promotes cell motility	1,40E-01
Defective SLC2A1 causes GLUT1 deficiency syndrome 1 (GLUT1DS1)	1,40E-01
Separation of Sister Chromatids	1,40E-01
Signaling by Interleukins	1,40E-01
Non-integrin membrane-ECM interactions	1,40E-01
Transcriptional regulation of granulopoiesis	1,40E-01
Mitotic Anaphase	1,40E-01
The role of GTSE1 in G2/M progression after G2 checkpoint	1,40E-01
Mitotic Metaphase and Anaphase	1,40E-01
Signaling by MET	1,40E-01
Metabolism of RNA	1,40E-01
Regulation of mRNA stability by proteins that bind AU-rich elements	1,40E-01
Lactose synthesis	1,40E-01
Transcriptional regulation of white adipocyte differentiation	1,40E-01
Type I hemidesmosome assembly	1,40E-01
EML4 and NUDC in mitotic spindle formation	1,40E-01

Appendix F: In vivo fatty acid concentrations

Table F.1 Median and quantiles for in vivo concentrations of BCFA in mg fatty acid/g feces of 174 samples from 12-month-old infants in the PreventADALL cohort. The concentrations were determined by GC, performed by Vitas (Oslo).

FATTY ACID	MEDIAN	2,5 % QUANTILE	97,5 % QUANTILE
C10	0,0149	0,0084	0,2599
C12	0,0582	0,0154	3,0673
C14	0,2309	0,0387	1,7813
C14:1c9	0,0099	0,0051	0,0230
C15	0,0694	0,0120	0,3143
C16	4,3969	1,1531	21,4247
C16:1c9	0,0460	0,0124	0,3453
C18	1,7723	0,3688	8,9196
C18:1c11	0,2188	0,0686	1,2494
C18:1c9	2,2962	0,5701	24,3510
C18:2n6	2,1011	0,3828	16,7373
C18:3n3	0,1245	0,0353	16,7462
C18:3n6	0,0374	0,0111	0,3555
C20	0,0934	0,0274	0,4010
C20:1n9	0,0834	0,0219	0,5612
C20:4n6	0,0283	0,0120	0,1096
C20:5n3	0,0137	0,0052	0,0669
C22/C20:3n6	0,1328	0,0479	0,4047
C22:5n3	0,0177	0,0080	0,1124
C22:6n3	0,0155	0,0056	0,0606
C24	0,1035	0,0426	0,2375
C24:1n9	0,0384	0,0134	0,1376
iso14	0,0153	0,0084	0,0769
iso15	0,0403	0,0090	0,1416
iso16	0,0183	0,0091	0,0970
iso17	0,0245	0,0092	0,0957
anteiso15	0,1236	0,0155	0,4787
anteiso17	0,0166	0,0060	0,0905
Unknown	1,3936	0,3469	5,2793
Sum FA	16,1299	4,6324	92,1577



Norges miljø- og biovitenskapelige universitet
Noregs miljø- og biovitenskapelige universitet
Norwegian University of Life Sciences

Postboks 5003
NO-1432 Ås
Norway